Genome-wide transcript and protein analysis reveals distinct features of aging in the mouse heart

Isabela Gerdes Gyuricza[1], Joel M. Chick[2], Gregory R. Keele[1], Andrew G. Deighan[1], Steven C. Munger[1], Ron Korstanje[1], Steven P. Gygi[3], Gary A. Churchill[1]

[1]The Jackson Laboratory, Bar Harbor, Maine 04609 USA;
[2]Vividion Therapeutics, San Diego, California 92121, USA;
[3]Harvard Medical School, Boston, Massachusetts 02115, USA

Corresponding author: gary.churchill@jax.org

ABSTRACT

Understanding the molecular mechanisms underlying age-related changes in the heart is challenging due to the contributions from numerous genetic and environmental factors. Genetically diverse outbred mice provide a model to study the genetic regulation of aging processes in healthy tissues from individuals undergoing natural aging in a controlled environment. We analyzed transcriptome and proteome data from outbred mice at 6, 12 and 18 months of age to reveal a scenario of cardiac hypertrophy, fibrosis, extracellular matrix remodeling, and reemergence of fetal gene expression patterns. We observed widespread changes in protein trafficking and sorting, and post-translational disruption of the stoichiometry of the protein quality control system itself. We identified genome hotspots of age-by-genetic effects that regulate proteins from the proteasome and endoplasmic reticulum stress response, suggesting that genetic variation in these modules may contribute to individual variation in the aging heart.

INTRODUCTION

Cardiovascular (CV) diseases are the leading cause of death in elderly people. Improved understanding of the mechanisms underlying the changes that occur in the heart with aging could open new opportunities for prevention and treatment (1). As the heart ages, characteristic physiological changes occur, including increased arterial thickening and stiffness, endothelium dysfunction, valvular fibrosis and calcification, and a switch from fatty acid to glucose metabolism (2–4). Compensatory mechanisms may temporarily maintain heart function but can also contribute to progressive deterioriation and eventual heart failure (2). Thickening of the left ventricle and remodeling of the extracellular matrix may compensate for the loss in systolic function (2,3). However, in the long term, the increased wall stress causes the left ventricle to dilate, leading to a decline in the systolic function (5).

Physiological measures of cardiac function that change with age, such as systolic blood pressure, have high heritability suggesting that genetic factors contribute to variability in aging (6). Linkage and association studies in humans have identified a number of candidate genes and pathways underlying age-related traits, though such studies have been limited by small sample sizes and confounding factors (6). Mouse models of aging recapitulate many of cardiac aging phenotypes in humans, such as increased atrial and ventricular dimensions and reduced diastolic function (7), and thus provide relevant tools for investigating aging processes in the heart. Recombinant mouse populations can be used to test the effects of specific genes on aging and lifespan (8). However, most previous studies have used mice descended from only a few isogenic strains that fail to capture the effects of genetic diversity found in human populations. The Diversity Outbred (DO) mouse population is derived from eight inbred founder strains: A/J (AJ), C57BL/6J (B6), 129S1Sv/ImJ (129), NOD/ShiLtJ (NOD), NZO/H1LtJ (NZO), CAST/EiJ (CAST), PWK/PhJ (PWK), and WSB/EiJ (WSB), representing genetic variation from classical and wild-derived strains and, as a result, display broad phenotypic diversity (9). The DO is a powerful tool for investigating the genetic drivers of aging due to its genetic and phenotypic diversity as well as its high mapping resolution.

Despite the well-known physiological alterations in the aging heart, dissecting their cellular and molecular basis is challenging due to its complex dynamics, resulting from the number of genes involved as well as contributions from environmental factors (8,10). Age-related cellular dysregulation has been associated with genomic instability, loss of protein homeostasis, epigenetic alterations, mitochondrial dysfunction and inflammation (10). The investigation of the molecular mechanisms involved in aging becomes even more complex due to the possible uncoupled nature of transcripts and their corresponding

proteins. Waldera-Lupa et al (2014) found that 77% of the proteins changing with age in human fibroblasts were not linked to changes in their corresponding transcripts (11). We also recently found that age-related changes in protein abundance in the kidney of DO mice are not driven by corresponding changes in their mRNA (Takemon et al., companion paper). These findings indicate that post-transcriptional regulation may play a substantial role in aging. In addition, there are reports in literature describing the increase of transcript expression variability with age in mammalian tissues, including the heart (12,13). The age-related dysregulation of some functional modules at the transcript level is accompanied by selective translation, therefore, the post-transcriptional machinery becomes crucial for achieving cellular homeostasis (14). For these reasons, investigating age-related changes using only transcriptional profiling may fail to reveal important influences on proteins and higher-order cellular processes.

In this study we analyze RNA-seq and mass-spec shotgun proteomics data from DO mice aged to 6, 12 and 18 months to uncover molecular changes in the heart that are associated with normal aging. At 6 months of age, the mice have reached full maturity. At 18 months, the majority of the mice are healthy and not showing signs of age-related decline. Thus, we are looking at changes in transcripts and proteins that are not influenced by developmental programs and are not reflecting late-stage disease progression (15). We examine broad patterns of change in biological processes and in specific cellular compartments using gene-set enrichment analysis (16). We examine the maintenance of protein-complex stoichiometry at both the transcript and protein levels (17). We leverage the genetic diversity of DO mice to identify loci that are associated with genotype-specific change with age in transcripts and proteins to better understand how genetic variation modulates age-related changes in the heart.

RESULTS

Transcriptomics reveals age-related changes in muscle cell differentiation, contraction, and inflammation

We identified transcripts that increase or decrease their expression with age in whole heart tissue from a cross-sectional sample of 192 DO mice. Both sexes were approximately equally represented across age groups of 6, 12 and 18 months. We found 2,287 transcripts (out of 20,932 total) whose expression changes with age (false discovery rate (FDR) < 0.1). A complete list of these transcripts is provided in Supplemental Table 1. The list of significantly changing transcripts confirms many genes that are known to play a role in the aging heart. We also identified genes that have been implicated in aging but have not been previously reported as changing in the heart, or they have been shown to play a role in heart disease or heart development but have not been reported to change with age. In total, the transcripts that change with age are enriched for functional annotations across 85 biological processes (FDR < 0.1), the most significant of which are muscle cell migration, regulation of muscle cell differentiation, ion transport pathways and acute-phase response (Figure 1).

Some of the transcripts possess functions relevant to cardiac pathological conditions and heart development (Table 1). *Myocd* is involved in both muscle cell migration and muscle cell differentiation pathways, and is an important regulator of cardiac function by maintaining cardiomyocyte cell structure and function (18). We observed a decrease in *Myocd* expression with age ($\log_2$ fold change per year of life (LFC) = -0.12). *Ppara* had decreased expression with age (LFC = -0.11), and plays a role in the regulation of cardiac fatty acid metabolism, contributing to several pathologic and physiologic heart conditions associated with aging (19,20). The gene *Adamts1 (*muscle cell migration pathway) has been described in cardiac aging (21) and, along with *Serpine1* (ion transport pathways), increases with age (*Adamts1*: LFC = 0.15; *Serpine1*: LFC = 0.19). These genes have been shown to induce collagen 1 deposition and fibrosis in the heart (21–23). *Nov* expression also increased with age (LFC = 0.18) and is known to participate in heart development, blocking terminal differentiation and increasing the proliferation rate of myoblasts (24,25). Many of the transcripts associated with ion transport that decrease with age are associated with calcium flow. These genes, including *Pln*, *Cacna1g* and *Dhrs7c*, have functions associated with cardiac muscle contraction, play a role in cardiomyopathy, and are downregulated in heart failure models, but have not been previously described in the aging heart (26–28).

Acute phase response pathway genes, which are involved in inflammation, all increase with age with the exception *Stat5b*, which decreases. Although its function in heart is not established, STAT5B interacts with the insulin receptor, coordinating changes in gene expression through insulin signaling in yeast and myosarcoma cells (29,30). In addition, STAT5B was proposed to inhibit acute-phase response by modulating the activation of STAT3 (31). Other transcripts in the acute phase response pathway that change with age include *Ahsg,* that controls the binding of free fatty-acid to inflammatory receptors and protects against vascular calcification (32,33), and *Tnfsf11*, which is involved in aortic valve calcification in response to inflammation, a feature prevalent in the elderly (34).

Enriched pathways for transcripts changing with age

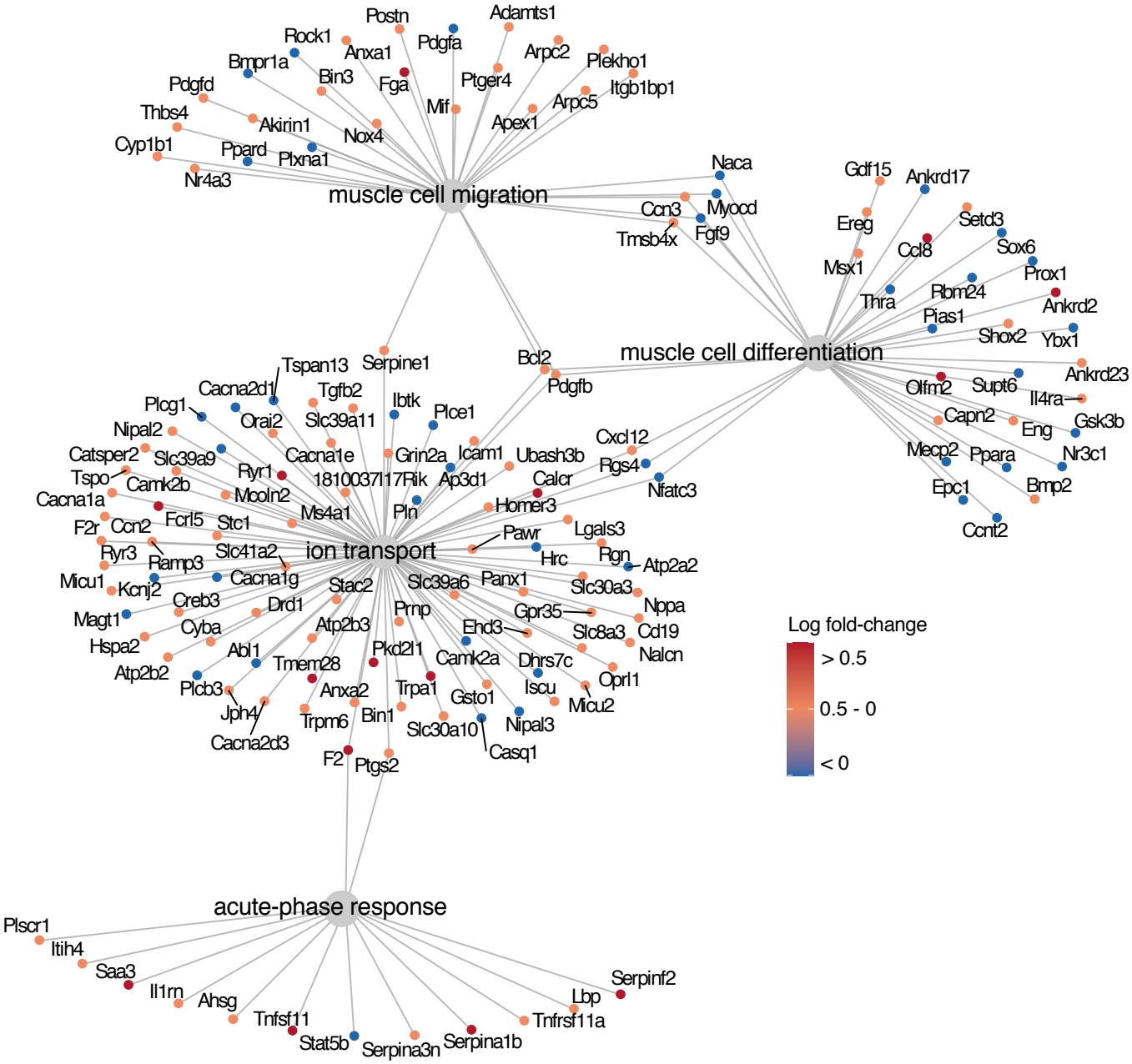

Figure 1. Most significant pathways showing age-related change in transcript expression. Gene-set enrichment analysis reveals that transcripts that change with age are involved in muscle cell migration, regulation of muscle cell differentiation, ion transport and acute-phase response (FDR < 0.1). Major nodes indicate enriched pathways and adjacent nodes correspond to transcripts that change with age within each pathway. Transcripts involved in muscle cell migration, muscle cell differentiation and ion transport increase and decrease with age (colors represent the LFC for each gene), while transcripts from the acute-phase response only increase expression with age with the exception of *Stat5b*.

Transcripts significantly changing with age

Table 1. Highlighted transcripts from differential expression with age analysis.

Transcript symbol	Direction of change	Function highlights	Reference index
Naca	Decreases	Sarcomere organization	(35–37)
Myocd	Decreases	Cardiomyocytes survival	(18)
Ppara	Decreases	Fatty acid metabolism	(38–40)
Adamts1	Increases	Cardiac fibrosis	(21)
Nov	Increases	Heart development	(24,25)
Olfm2	Increases	Vascular smooth muscle cell regulation	(41)
Cacna1g	Decreases	Cardiac muscle contraction	(42,43)
Pln	Decreases	Cardiac muscle contraction	(26)
Serpine1	Increases	Cardiac fibrosis	(22,23)
Bcl2	Increases	Antiapoptosis	(44)
Stat5b	Decreases	Insulin signaling	(29,30)
Ahsg	Increases	Free fatty-acid signaling	(32)
Tnfsf11	Increases	Aortic valve calcification	(34)

Proteomics reveals age-related changes in mitochondrial metabolism and intracellular protein transport

Of 192 DO mice with transcript data, we were able to obtain proteomics data from 190. We detected 1,161 proteins (out of 4,062 total) that change with age (FDR < 0.05). A higher proportion of proteins exhibited change with age when compared to transcripts, and thus we used a stricter FDR threshold to focus on the proteins with greatest change. These proteins are enriched for the following gene ontology terms (FDR < 0.05): positive regulation of cellular proliferation, intracellular protein transport and several mitochondria-related pathways (Figure 2). These pathways included proteins that both increased and decreased with age. None of the enrichment terms for proteins overlap with those found in the transcriptome analysis. Thus, the protein data are able to reveal unique features of the aging process that are not seen in the transcript level. A complete list of proteins that change with age is provided in Supplemental Table 2.

The enrichment categories associated with mitochondria include proteins from the cytochrome C oxidase (COX) complex, i.e. the mitochondrial respiratory chain complex IV, which all increase with age (COX6B1: LFC = 0.4; COX4L1: LFC = 0.3). We quantified protein levels for 16 COX subunits of which 13 show increased abundance with age, suggesting an increase in oxidative mitochondrial metabolism (Supplemental Table 2). Interestingly, the ACTN3 protein decreases with age (LFC = -1.8). ACTN3 (alpha-actinin-3) has not been described in the heart before, but its role is well documented in skeletal muscle, where it regulates oxidative metabolism (45,46). Studies show that depletion of ACTN3 results in overexpression of COX proteins and consequently leads to higher mitochondrial oxidative metabolism (45,46), which is consistent with the relationships we observe. Complexes I, II and III of the mitochondrial respiratory chain also reveal age-related changes. Proteins from the UQCR (ubiquinol-cytochrome c reductase complex – Complex III) and SDH family (succinate dehydrogenase complex – Complex II) all increase with age (UQCR10: LFC = 0.57; UQCRH: LFC = 1.0; SDHC: LFC = 0.67; SDHD: LFC = 0.6). In contrast, subunits from the mitochondrial complex I, such as NDUF (NADH: ubiquinone oxidoreductase supernumerary subunits – Complex I), both increase and decrease with age (NDUFB6: LFC = 0.18; NDUFV3: LFC = 0.46; NDUFA1: LFC = -1.1; NDUFAB1: LFC = 0.55).

The proteins AKT1 and AKT2 are serine/threonine kinases highly abundant in cardiomyocytes and regulate cellular proliferation and intracellular protein transport pathways. Both are significantly increasing their abundance with age (AKT1: LFC = 0.36; AKT2: LFC = 0.27). AKT1 and AKT2 respond

differently to growth factors and extracellular ligands (47), but they both participate in the regulation of cardiac hypertrophy in aging through interaction with Sirtuins (48). Knockout mouse models have shown that the lack of AKT1 constrains the ability of cardiomyocytes to respond to physiological hypertrophy. Alternatively, AKT2 mutant mice showed reduced glucose oxidation in heart cells, but normal response to exercise-induce hypertrophy, demonstrating that these two proteins regulate heart remodeling response to stress in distinct ways (47,49,50). Along with AKT2, other proteins associated with fetal metabolism also increase with age, including ACACB (Acetyl-CoA Carboxylase Beta), which inhibits fatty acid oxidation, and GYS1, which plays a role in glucose metabolism (49,51,52).

Proteins from the RAB family are Ras-like GTPases that regulate protein trafficking by vesicle formation and fusion throughout the cell (53,54). Among the 22 RAB proteins that change with age, 19 are increasing (Supplemental Table 2). Some RAB proteins are activated during mitophagy, which is mediated by RABGEF1 in mammalian cultured cells (55). Notably, RABGEF1 is the RAB family member with greatest age-related abundance increase (LFC = 0.74), suggesting that mitophagy may play a substantial role in the aging heart. Increased myocardial RAB abundance is associated with myocardial hypertrophy. Mice overexpressing RAB1A showed contractile depression with impaired calcium reuptake and developed hypertrophy that progressed to heart failure (53). RAB1A and RAB1B are mostly identical in terms of both structure and function (56) and RAB1B is one of the few RAB proteins that decreased with age in our dataset (LFC = -0.356).

Enriched pathways for proteins changing with age

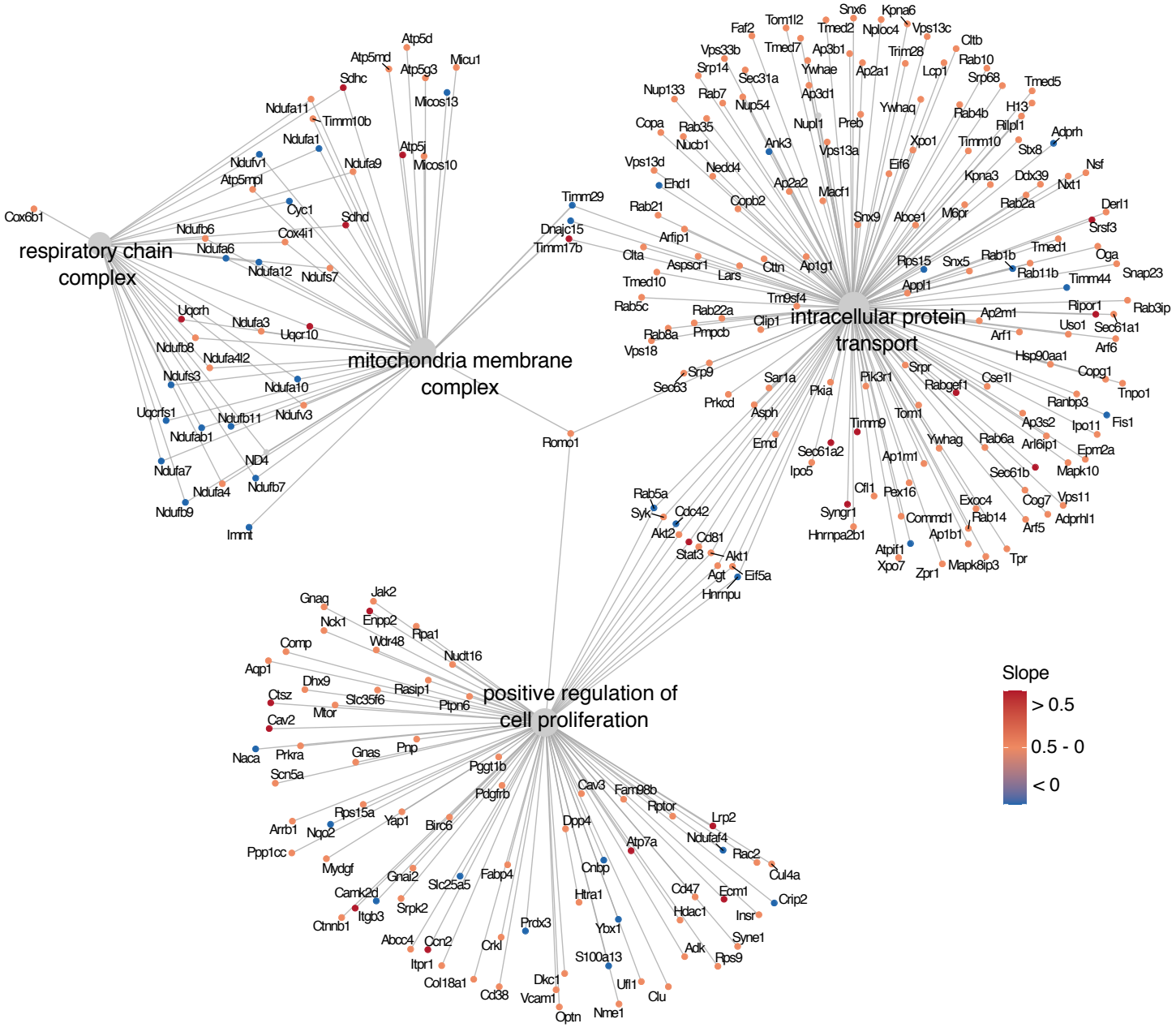

Figure 2. Pathways showing age-related change in protein abundance. Gene-set enrichment analysis reveals that proteins changing with age are involved in positive regulation of cell proliferation, intracellular protein transport, mitochondria membrane complex and respiratory chain complex (FDR < 0.1). Major nodes indicate enriched pathways and adjacent nodes correspond to proteins identified within each pathway. The majority of proteins increase their abundance with age (colors represent the $\log_2$ fold change per year (LFC)), notably including proteins involved in intracellular protein transport and positive regulation of cell proliferation.

Proteins significantly changing with age

Table 2. Highlighted proteins from differential abundance with age analysis.

Protein symbol	Direction of change	Function highlights	Reference index
CRIP2	Decreases	Smooth muscle tissue differentiation and cardiomyocyte survival	(57–59)
ATP1F1	Decreases	Inhibition of mitochondrial ATPase activity	(60,61)
TIMM29	Decreases	Translocase of inner mitochondrial membrane (Complex 22)	(62)
AKT1	Increases	Physiological cardiac growth	(47,49)
AKT2	Increases	Cardiac glucose metabolism	(47,50)
ACTN3	Decreases	Muscle anaerobic metabolism	(46)
UQCRH	Increases	Mitochondrial respiratory chain complex III cytochrome b subunit	(63)
SDHD	Increases	Mitochondrial respiratory chain complex III cytochrome b subunit	(64)
COX4I1	Increases	Mitochondrial respiratory chain complex IV cytochrome c subunit	(65)
NDUFB6	Increases	Mitochondrial respiratory chain complex I subunit	(66,67)
NDUFA1	Decreases	Mitochondrial Respiratory Chain Complex I subunit	(68)
RABGEF1	Increases	Mitophagy induction	(55)

Dysregulation of protein-complex stoichiometry with age

Loss of stoichiometry in protein complexes has been shown to occur with age in a number of organisms (69,70). We asked how the balance of component proteins in key age-related complexes was regulated at both the transcript and protein level. Based on protein-complex definitions from the CORUM database (71), we identified 16 complexes likely associated with the aging process and whose transcripts and proteins are present in our dataset (26S proteasome, nuclear pore complex, cytoplasmic ribosomal small subunit, cytoplasmic ribosomal large subunit, mitochondrial ribosomal large subunit, coat protein I (COPI) vesicle transport, coat protein II (COPII) vesicle transport, mitochondrial ribosomal small subunit, mitochondrial respiratory chain complexes (I-V), mitochondrial pyruvate dehydrogenase complex, mitochondrial inner membrane presequence translocase complex, mitochondrial outer membrane translocase complex). We computed the Pearson correlations between all pairs of genes, at the protein and transcript levels, for each complex, and then estimated the age trend for each gene-pair correlation coefficients (Methods). We evaluated the significance of the age trends using a permutation procedure (17).

At the protein level, we observed 123 gene-pairs out of 2074 whose correlations significantly change with age (FDR < 0.1) (Supplemental Table 3). Of which, 81 are in the 26S proteasome complex, 4 are in the cytoplasmic ribosomal small subunit complex, 11 are in the COPII complex, and 27 are from the mitochondrial respiratory chain complexes (5 from mitochondrial complex I, 2 from mitochondrial complex II, 5 from mitochondrial complex III, 4 from mitochondrial complex IV and 11 from the mitochondrial complex V). The majority (115 out of 123 pairs) of correlations decrease with age at the protein level, suggesting a loss of stoichiometric balance in these complexes.

At the transcript level only 20 out of 2042 pairs showed significant change with age (FDR < 0.1), and all of them are part of mitochondrial complexes (3 from mitochondrial complex III, 15 from mitochondrial complex V, and 2 pairs from the mitochondrial pyruvate dehydrogenase complex). Interestingly, all of these pairs increase their correlation with age (Supplemental Table 3). Only two of these gene-pairs showed a significant change at the protein level as well (*Atp5*b – *Atp5a1* Mitochondrial complex V: protein age regression coefficient (estimate) = -0.03; transcript estimate = 0.02, and *Uqcrc2* – *Uqcrh* Mitochondrial complex III: protein estimate = 0.03; transcript estimate = 0.02). The figure 3(A-D) summarizes the age-trend findings for the 26S proteasome complex.

In order to capture the whole picture of how the correlations change with age for each protein complex, we adjusted the modeling strategy. Considering that testing for age trends for each gene-pair comparison could fail in revealing major changes for the protein complexes, we also fit the overall correlation age trend for each complex, at both the transcript and protein levels, without testing for each gene-pair individually (Methods). The same permutation method was used to address the statistical significance (Methods).

We found that the mitochondrial complex III is the only complex in which the overall correlations change only at the transcript level (transcript estimate = 0.02), while the complexes mitochondrial outer membrane translocase (protein estimate = -0.02), nuclear pore complex (protein estimate = -0.01), cytoplasmic ribosomal large subunit (protein estimate = -0.006) and 26S proteasome (protein estimate = -0.02) showed changes only at the protein level (Figure 3E). In addition, we found that the mitochondrial complexes IX and V change their correlations, for both transcript and protein levels, at the same rate (transcript estimate ˜ 0.02; protein estimate ~ -0.01). Despite the fact that nine complexes did not show a significant change ($p < 0.05$) in the overall correlation with age, the majority of them mapped on the low right corner of the plot (Figure 3E), which indicates a positive age trend at the transcript level, but a negative age trend at the protein level. This corroborates our previous findings for the gene-pair comparisons, in which the pairwise correlations tend to increase with age at the transcript level, but decrease at the protein level (Figure 3A-D). Furthermore, the decrease observed at the protein level for the 26S proteasome complex is notably larger than the other complexes, revealing that this complex might be the one that is mostly affected in the aging process.

Protein correlation plots and age trend

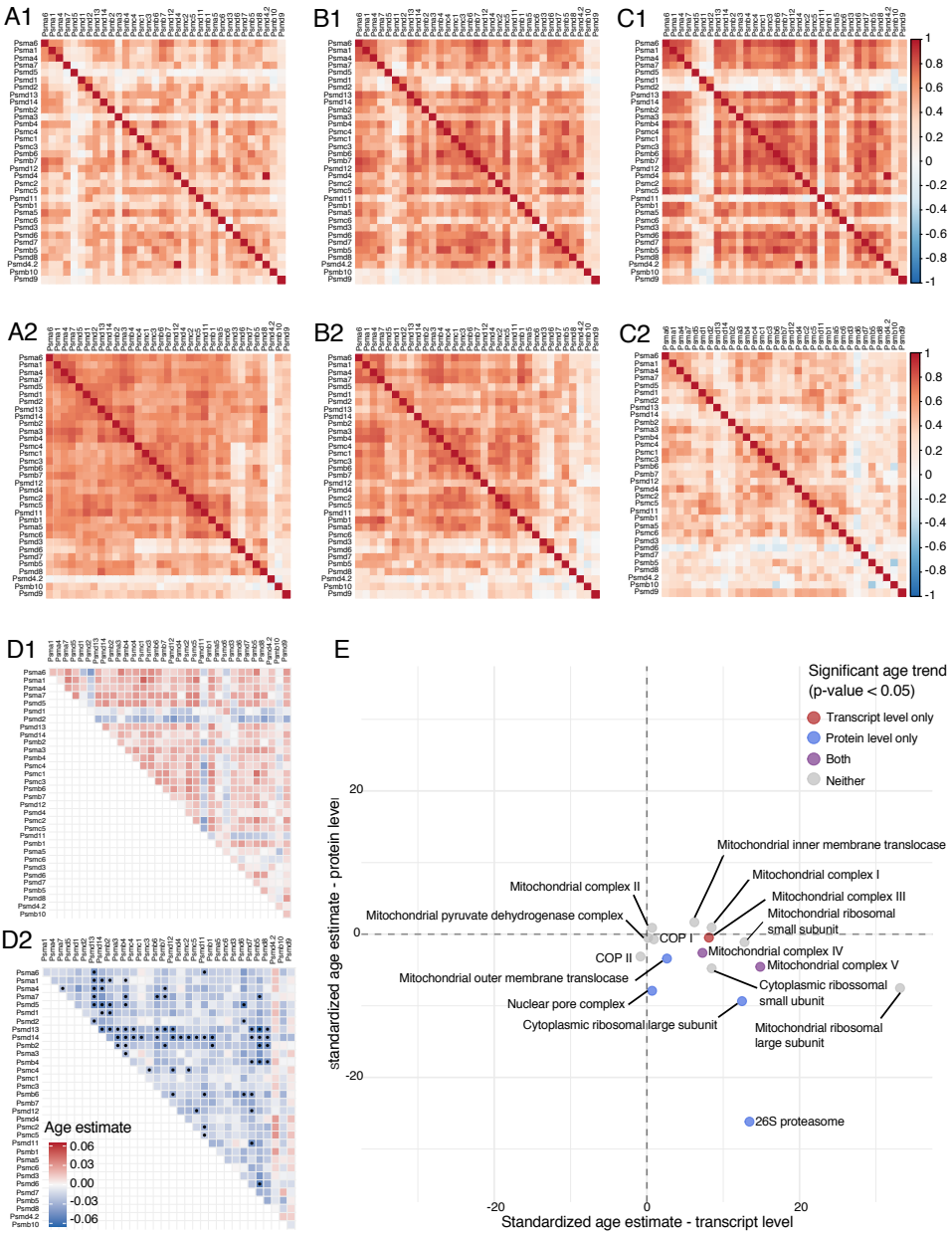

Figure 3. Heatmaps of the correlation coefficients between pairs of genes in the 26S proteasome complex at 6 months (A), 12 months (B) and 18 months (C) at the transcript level (1) and at the protein level (2). D) Heatmaps for the age trend in correlations between members of the 26S proteasome complex show that correlations at the transcript level are generally increasing with age but are not statistically significant (D1). At the protein level (D2) the majority of correlations are decreasing with age. Dots indicate significant age-trend for the pairwise correlations with age (FDR < 0.1). E) Standardized estimates of the change in correlation with age for all the protein complexes at the transcript (x-axis) and protein (y-axis) levels. Color indicates the significance of the age trend at the transcript level, protein level, both or neither. Even though many of the complexes do not show a significant trend with age, it is interesting to note that, in general, their age estimates tend to increase at the transcript level, but decrease at the protein level.

Genetic variants alter the age trajectory of functionally related groups of proteins

We carried out genetic mapping analysis of transcripts and proteins to identify quantitative trait loci (eQTL and pQTL, respectively) that regulate their expression/abundance levels. The additive effects of genetic variation on transcripts and proteins have been widely studied and documented (72–76) and it will not be discussed here. Our interest is to investigate how genetic variants influence the rate or direction of change with age of transcripts and proteins. To identify these age-interactive QTL (age-QTL), we evaluate an age-by-genotype interaction term in a linear mixed model of genetic effects (Methods) for each transcript and protein. We computed genome-wide adjusted significance using a permutations strategy (Methods) and declare age-QTL when the age-interactive LOD score (LOD_{int}) > 7.75. We have provided access to the data and webtools that can be used to explore both the additive and age-interactive genetic effects on transcripts and proteins in the aging mouse heart (https://churchilllab.jax.org/qtlviewer/JAC/DOHeart).

We found 824 significant transcript age-QTLs (age-eQTL). These are primarily mapped to locations that are distant from the coding genes, which implies that age-related changes are, largely, not a function of direct regulation of gene expression and are rather a response to other age-related changes. Only 5 of the age-eQTL are local. A local age-eQTL for the gene *Cluh* (LOD_{int} = 7.9) is located on chromosome 12. This gene binds RNAs of nuclear-encoded mitochondrial proteins, regulating mitochondrial metabolism by translation control and mRNA decay (77,78). Interestingly, *Cluh* is also crucial in orchestrating mitochondrial metabolic switches, such as the shift from glycolysis to oxidative phosphorylation that happens after birth (78). Genetic variation in *Cluh* might influence the return to the fetal metabolism in the aging heart.

For proteins, we found 463 significant protein age-QTLs (age-pQTL), none of which are local to the coding gene. The protein PARK7 mapped a distal age-pQTL on chromosome 9 (LOD_{int} = 10.5) at ~95Mb. PARK7 is a redox-sensitive chaperon that protects the murine heart from oxidative damage (79). SIRT2, another protein with relevant function to the aging heart, has a distal age-pQTL on chromosome 13 at ~111Mb (LOD_{int} = 9.6). SIRT2 regulates cardiac homeostasis and remodeling through activation of AMP-activated protein kinase (AMPK) and repression of the nuclear factor of activated T-cells (NFAT), playing a protective role in the heart (80,81).

Genomic hotspots for age-interactive eQTL and pQTL

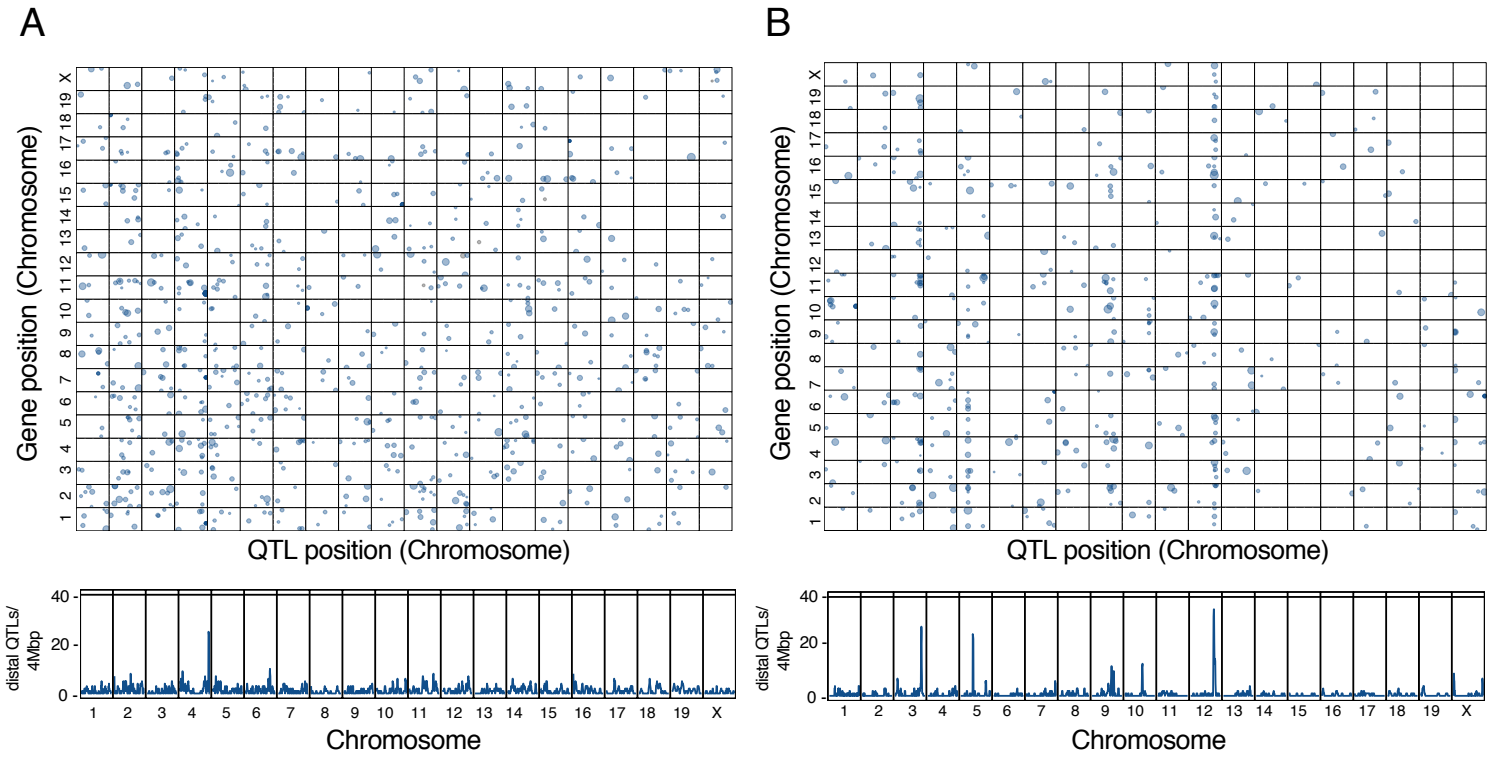

Figure 4. Age-by-genetic effects are predominantly non-local and map to distinct hotspot region that affect many transcripts and proteins. Age-QTL are mapped by testing an age-by-genotype interactive term in genome scans for each transcript and protein. At these loci, the DO founder haplotypes influence the rate or direction of change with age of transcript or protein expression/abundance. Distal QTL hotspots represent small genomic regions where several transcripts or proteins have age-QTL at the same locus. Genetic variation at hotspot loci regulate the age-related dynamics of multiple transcripts or proteins. Hotspots for the significant QTLs (LOD_{int} > 7.75) appear as vertical bands (upper panel) and peaks (lower panel).

We observed that many age-QTLs co-locate to the genome in hotspots. We identified an age-eQTL hotspot on chromosome 4 and three age-pQTL hotspots on chromosomes 3, 5 and 12, respectively (Methods). Genome-wide significant age-QTL meet stringent statistical criteria that can result in missing weaker but biologically relevant age-QTL. Therefore, at each hotspot, we also considered transcripts or proteins with suggestive QTL ($LOD_{int} > 6$). We then computed the correlation of all candidate transcripts or proteins within each hotspot and retained only those with absolute mean correlation greater than 0.3. This filter removed genes with age-QTL that are not tightly correlated with other genes at the hotspot and thus less likely to share common genetic regulators. For the age-eQTL hotspot on chromosomes 4, none of the transcripts met this criterion suggesting that the hotspot genes are regulated by multiple independent genetic variants. However, all three age-pQTL hotspots included highly correlated proteins, with 130 at the chromosome 3 locus, 110 at the chromosome 5 locus, and 161 proteins at the chromosome 12 locus (Supplemental Figure 1 and Supplemental Table 4).

To determine if the proteins that map to the age-pQTL hotspots share common biological functions, we performed enrichment analysis. The proteins in the chromosome 3 hotspot are enriched (FDR < 0.05) for genes in the proteasome complex, including proteins from the PSM family (a subunit of the proteasome complex); myosin filament, including proteins such as MYH6 and MYH3 that are responsible for muscle cell structure; and the nucleosome pathway, composed by members of the histone families H1, H2 and H3 (Figure 5A). The proteins that mapped to the chromosome 5 hotspot are associated with a variety of pathways (24 in total with FDR < 0.05), but the two most significant are the endoplasmic reticulum lumen pathway, composed of proteins of the endoplasmic reticulum stress response, such as PDIA4, HSPA5 and HSP9B1, and the contractile fiber pathway containing proteins associated with the muscle contraction apparatus, such as Titin and Desmin (Figure 5B). Finally, for the chromosome 12 hotspot, we found more than 40 significant pathways (FDR < 0.05) for which the most significant one is the muscle contraction pathway that includes proteins related to muscle cell organization, such as myosins and actin, as well as proteins involved in calcium transportation (CACNA2D1) and mitochondria energy generation (NDUFS6) (Figure 5C). Another pathway that was highly significant is the non-coding RNA (ncRNA) transcription pathway, associated with chromatin organization, and includes histone H2 family members and a histone chaperone (NPM1) (Figure 5C).

Enriched pathways for proteins in the age-pQTL hotspots

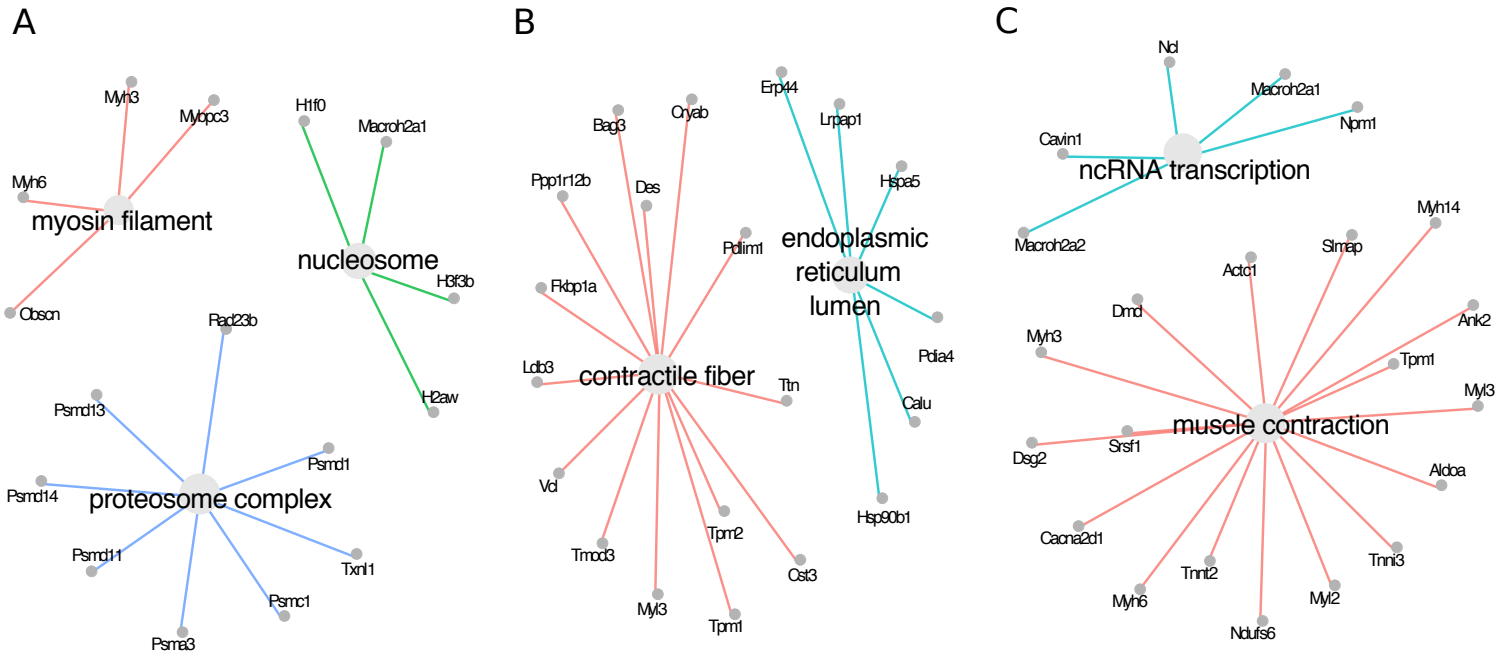

Figure 5. Most significant pathways for proteins mapping to the age-pQTLs hotspots. Enrichment analysis shows that the three hotspot regions each regulate proteins involved in distinct biological processes. Proteins that map to the chromosome 3 hotspot (A) are primarily associated with myosin filament, nucleosome and proteasome complex, while proteins that map to the chromosome 5 hotspot (B) participate in contractile fiber and endoplasmic reticulum lumen. Proteins that map to the chromosome 12 hotspot (C) are associated with muscle contraction and ncRNA-transcription.

To investigate how change in protein abundance with age can vary due to genetic factors, we estimated the age-specific effects of each DO founder haplotype on the first principal component (PC 1) of the proteins that mapped to each hotspot (Figure 6). Each hotspot had a distinct pattern of founder allele effects. For the hotspot on chromosome 3, the effects of the B6 and PWK alleles exhibit clear opposing trends with age (Figure 6A). For chromosome 5, the effect of the AJ allele on protein abundance shows a pronounced trend with age compared to the other founder alleles (Figure 6B). At the chromosome 12 hotspot, the magnitude of the effects of 129 and NOD alleles increase with age, but in opposite directions (Figure 6C).

We confirmed these effects for individual proteins that mapped to the hotspots, considering that proteins that are positively correlated to each other have similar allele effects and proteins that are negatively correlated show the opposite direction of change (Figure 6). The chromosome 3 hotspot includes members of the histone families (H2AFY and H3F3B), that participate in chromatin structuring and are positively correlated (Supplemental Table 4). For these proteins, B6, CAST or WSB alleles drive decreasing abundance with age, while the PWK allele has the opposite effect (Figure 6A).

Proteins HSPA5 and PDIA4, that mapped to the chromosome 5 hotspot, participate in the physiological endoplasmic reticulum (ER) stress response and are positively correlated (Supplemental Table 4). These proteins and others involved in ER stress response are negatively correlated with TTN, a protein responsible for sarcomere structuring and muscle contraction. For mice with the A/J allele, HSPA5 and PDIA4 increase with age and TTN abundance decreases with age (Figure 6B).

The chromosome 12 hotspot includes proteins related to chromatin structuring, such as H2AFY (that also mapped to the chromosome 3), H2AFY2 and NPM1. The histones proteins, H2AFY and H2AFY2, are positively correlated to each other and display similar allele effects, in which the 129 allele induces a decrease in abundance with age. The protein NPM1, which encodes a histone chaperone, is negatively correlated to both H2AFY and H2AFY2 and shows opposite allele effects (Figure 6C).

Since distal QTL hotspots represent genetic variation that locally effect an intermediate gene that regulates many downstream targets, we looked for genes within the intervals of the hotspots that could be the genetic drivers. Contiguous to the hotspot on chromosome 3 (145 – 150Mb), we identified a non-significant local pQTL (LOD_{int} = 7) for the protein SH3GLB1, known as BIF-1. The gene is located between 144.68 – 144.72Mb and has a similar age-by-genotype effects pattern to the PC 1 (Figure 6A). In addition, BIF-1 plays a role in autophagy regulation (82,83), an important component of protein quality control

system that was shown in multiple studies to decline with age (84). Even though the local pQTL for BIF-1 did not show statistical significance, the additional biological information supports it as a potential candidate driver for the age-related changes in proteins that mapped to the chromosome 3 hotspot.

Allele effects of founder haplotypes on protein abundance at age-interactive pQTL hotspots

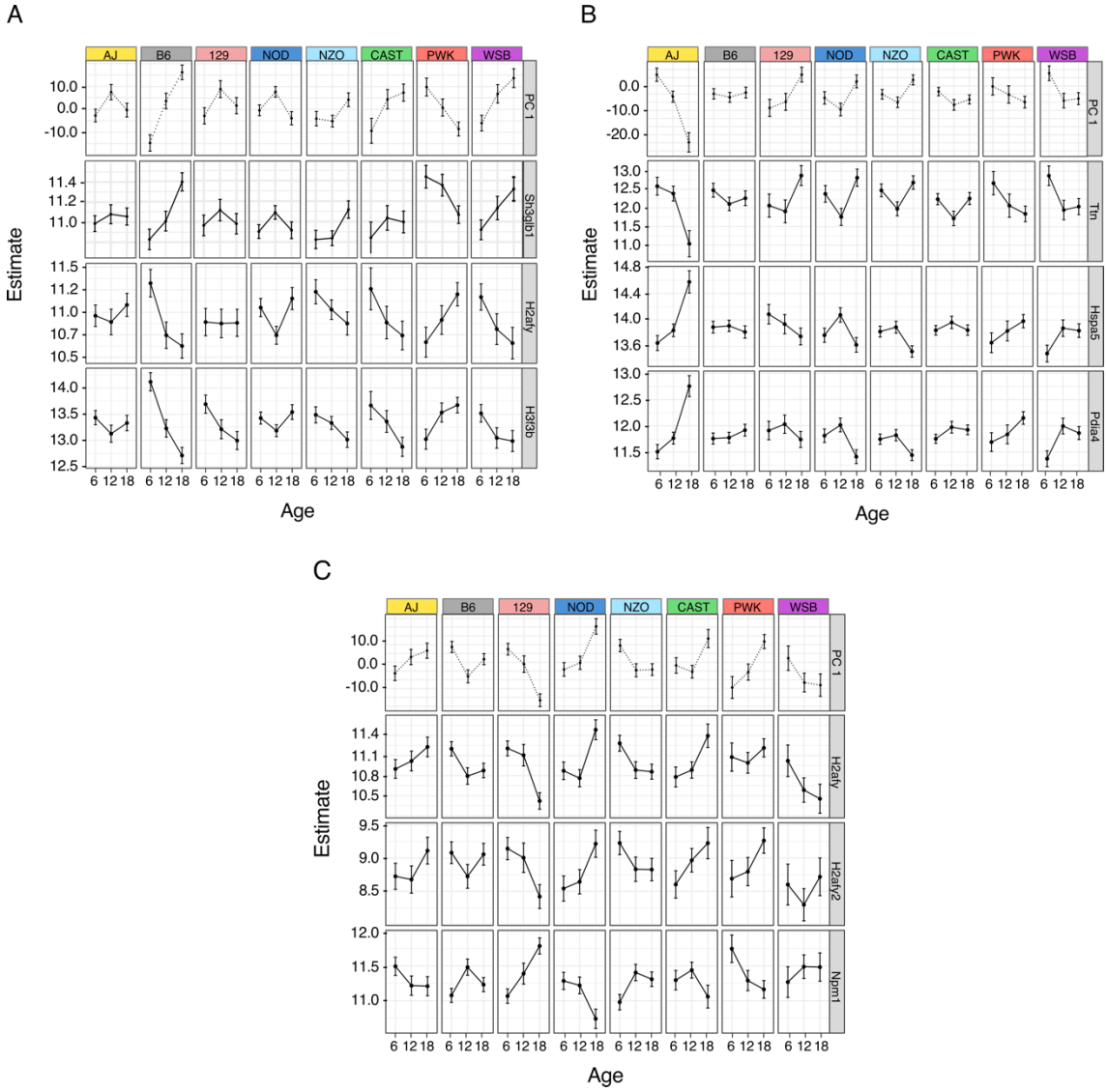

Figure 6. Founder allele effect changes with age for the first principal component (PC 1), representing a hotspot summary, and for selected individual proteins that mapped at each age-pQTL hotspot. Proteins H2AFY and H3F3B in the chromosome 3 hotspot participate in the same biological process (nucleosome complex) and are positively correlated to each other, and so share the same directionality of change with age (A). Protein SH3GLB1, that also mapped to the chromosome 3 hotspot, is negatively correlated to H2AFY and H3F3B, and thus has inverted alleles pattern when compared to these proteins (A). In addition, the allele effects of each founder for SH3GLB1 and for the PC 1 are quite similar, suggesting SH3GLB1 as a candidate genetic driver (A). HSPA5 and PDIA4 mapped age-pQTL to the chromosome 5 hotspot and they participate in the endoplasmic reticulum stress response. These proteins are positively correlated to each other, thus possess a similar alleles effect pattern (B). These proteins are negatively correlated to TTN, involved in sarcomere structure, and so, show opposite allele effects (B). H2AFY and H2AFY2, both associated with chromatin structuring, mapped age-pQTL to the chromosome 12 hotspot, and are positively correlated to each other, sharing similar allele effects pattern (C). These proteins are negatively correlated to NPM1, also involved in chromatin structure (histone chaperone), thus they show opposing directions of allele effects with age (C).

DISCUSSION

By analyzing both the transcriptome and the proteome of the aging mouse heart we were able to detect distinct biological processes that are altered through the course of natural aging. We found that transcriptional changes with age are not necessarily followed by a change in their corresponding proteins and likewise, changes with age in proteins are not preceded by corresponding transcriptional changes. Our analysis reveals that transcripts decreasing in expression with age are associated with cardiomyocyte contraction and survival, and fatty-acid metabolism. These findings are consistent with previous reports describing disrupted Ca2+ handling, progressive loss of myocytes, and metabolism switch in the aging heart, which may reflect a compensatory mechanism to improve contractility (3,4,85). Transcripts increasing their expression with age are involved in the acute-phase response and cardiac fibrosis, which suggest chronic inflammation and loss of cardiomyocytes that stimulate extracellular matrix remodeling during the aging process (86–88).

Proteomics reveals major features of the aging heart that are not detected at the transcript level. We saw changes in mitochondrial respiratory chain proteins, as well as intracellular protein and vesicular transport pathways, in agreement with previous proteome analysis of the aging mouse heart (89,90). We observed that most of the proteins from the RAB and AKT families increase their abundance with age, suggesting physiological growth of cardiomyocytes and increased cellular synthesis, which is commonly observed in hypertrophic hearts (1). Proteins of the mitochondrial respiratory complexes II, III and IV increase with age while proteins from Complex I change in both directions. It seems likely that the up-regulation of proteins from the other mitochondrial complexes acts as a compensatory mechanism in response to an input deficiency from early steps in oxidative phosphorylation.

We also found that the abundance of protein ACTN3, involved in the structuring of sarcomeric Z line and the regulation of the contraction apparatus, decreases with age. *Actn3* expression has been observed in the skeletal muscle, but has not been reported previously in the heart of either mice or humans (91). In knockout mice, the deficiency of ACTN3 in the skeletal muscle promotes a switch from fast-anaerobic metabolism towards a more efficient aerobic metabolism, leading to better exercise performance (45,46). The same study also speculated that the *Actn3* null allele has been under positive selection in modern humans, suggesting that aerobic metabolism boosting may confer a fitness advantage (46). In humans, ACTN2 and ACTN3 appear to have functional redundancy, and *Actn2* was recently linked to heart failure in a multi-omic analysis (91,92). Our data suggests that ACTN3 may participate in the

regulation of metabolic efficiency not only in the skeletal muscle, but also in the mouse heart, and might contribute to the physiological changes in muscle efficiency during the aging process.

We observed that proteins associated with fetal metabolism increase with age. A return to embryo/fetal gene program occurs in some pathological heart conditions and it is thought to play a protective role (93,94). The fetal heart is under constant stress conditions, including hemo-dynamic load and hypoxia, and thus uses carbohydrates as a primary energy source to maintain cardiac efficiency (93,95). The aging heart also undergoes different types of stress including the accumulation of reactive oxygen species, cardiomyocyte loss, mitochondria dysfunction and possibly hypoxia (85,96). These stressors are even more pronounced when they co-occur with other age-related comorbidities, such as diabetes mellitus and hypertension. Studies have demonstrated a return to the fetal gene program in diabetic rats with cardiac diseases (97,98). We propose that a return to the fetal program also happen in mice during the normal aging process and may play an adaptive role to compensate for decline in other biological functions of the heart.

The protein data revealed changes in the balance between members of protein-complexes with age. In general, the correlations between proteins within complexes decrease with age. In contrast, correlations at the transcript level tended to increase with age, although these trends were less pronounced. This dynamic suggests that stochiometric regulation in protein-complexes is largely post-transcriptional, and it seems plausible that changes at the transcript level could be a compensatory effect to balance the age-related erosion of regulation at the protein level. This is largely consistent with previous studies that have shown that the production of protein-complex subunits is not always perfectly stoichiometric and post-translational mechanisms play an essential role in removing extra subunits and promoting the balance of these complexes (70).

In addition, several studies also showed that aging and the progressive decline of the proteasome activity can lead to a loss of protein-complex stoichiometry and increased protein aggregation (99–101). Here, we show an age-related decline in the correlation between protein subunits from mitochondrial complexes, suggesting that loss of stoichiometry may contribute to mitochondrial dysfunction in the aging heart. This finding is further corroborated by the observed changes in abundance of members of the mitochondrial Complex I described earlier, in which some proteins increase their abundance with age, while others decrease. However, the most striking finding is the observed loss of stoichiometry in the 26S proteasome and the COP II complexes, which, likely disrupts the processes of protein trafficking and sorting in the cell. The proteasome system plays a crucial role in regulating the abundance and

stoichiometry of proteins in the cell (102), and several studies have attempted to understand why proteasome activity declines with age (103). Here, we show that aging disrupts the regulation of the proteasome system itself, which, potentially, contributes to a vicious cycle of progressive protein quality control breakdown during the aging process.

We found age-pQTL hostpots that modulate the dynamics of proteins involved in protein quality control. Most of the age-QTLs found were distal, indicating that the genetic variation has a weak age-effect on the regulation of its proximal genes, which further supports the importance of post-transcriptional mechanisms in regulating homeostasis during aging (11,14). The implication is that genetic variation is directly influencing one or more genes at the hotspot locus. In turn these gene products interact in higher-order molecular networks that influence age-related changes of functionally related groups of proteins.

Enrichment analysis of the hotspots on chromosomes 3 and 5 identified proteins that function in the proteasome complex and endoplasmic reticulum (ER) lumen, respectively (Figure 5A/B). These modules are part of the protein quality control system that coordinates proteostasis and cell survival (104). The ER contains transmembrane proteins that sense the presence of misfolded proteins, which then activates transcription factors that up-regulate the expression of ER stress response genes (104). Some misfolded proteins are marked by ubiquitination and transferred to the cytosol, where they are degraded by the proteasome complex (104). The proteins HSPA5, HSP90B1 and PDIA4, present in the chromosome 5 hotspot (Figure 5B), are known to be downstream targets of the ATF6 branch of the ER unfolded protein response and this pathway was found to be adaptive and cardioprotective in several studies (105–108).

Enrichment analysis of the hotspots on chromosomes 3 and 12 identified proteins associated with chromatin structure (Figure 5), including histones and histones chaperones, such as NCL and NPM1 (Figure 6C). Loss of chromatin structure was previously reported in aging models for yeast and human fibroblasts (109,110), and leads to dysregulation of global gene expression, increased genomic instability, and promiscuous access of DNA damaging agents to the chromatin (111,112). It is interesting to note that all histone proteins in our data decrease with age (Supplemental Table 2), suggesting that a loss of chromatin structure with age also occurs in the heart.

Proteostasis decline and chromatin structure loss are known to occur in the aging process. We found that genetic variation in different regions of the genome might alter the trajectory of these events, demonstrating that each founder strain allele of the DO mice contributes in a specific way, and sometimes

in opposite ways, to protein abundance changes with age. For example, while the B6 allele at chromosome 3 (between 145 and 150Mb) seems to induce a decrease in the abundance of histones H1F0, H2AFY and H3F3B with age, the PWK allele at this same locus has the opposite effect on these proteins.

We identified the protein SH3GLB1 (BIF-1) as a potential driver of the age-related dynamics of proteins that mapped at the chromosome 3 hotspot. SH3GLB1 is a member of endophilin protein family that plays a role in mitochondrial fission, vesicle formation and autophagy (82,113,114). As mentioned earlier, the protein quality control system contributes to the aging process and studies suggest that increased autophagy may be a compensatory effect when the proteasome complex is disrupted (115,116). In addition, autophagy plays an important role in maintaining chromosomal stability, and loss of both *Sh3glb1* and its associate *Beclin-1* were shown to induce DNA damage due to metabolic stress (117,118). Autophagy is crucial for maintaining cardiac function - mice with disrupted autophagy show anomalies in sarcomere and mitochondria structure (119). Our findings suggest that genetic variation among the founder strains near the *Sh3glb1* locus influences individual rates of change with age of proteins involved in the proteasome complex, chromatin structuring and muscle apparatus organization.

In summary, we have described changes that occur with normal aging in heart tissue from DO mice that suggest a scenario of mitochondrial dysfunction, physiological hypertrophy, and a return to the fetal gene expression program. The proteome data revealed aspects of aging in the heart that are not seen at the transcript level, including the remarkable loss of stoichiometry of protein-complexes involved in protein trafficking and sorting. This finding suggests that the proteasome disruption itself may play a causal role in the progression of protein quality control breakdown during the aging process. The contribution of the protein quality control system in the aging heart is further demonstrated by the identification of age-pQTL hotspots that modulate abundance of proteins involved in the proteasome and the ER stress response, demonstrating how genetic variation acts on functional modules and contributes to individual variability in the aging heart.

MATERIAL AND METHODS

Study cohort and tissue collection

The initial cohort consisted of 600 DO mice (300 of each sex) bred at The Jackson Laboratory (stock no. 009376) across five waves (representing generations 8-12 of the DO). Mice were maintained on a standard rodent chow (LabDiet 5K52, St. Louis, MO) in an animal room that was free of pathogens, had a set temperature ranging from 20-22°C, and a 12-hour light/dark cycle. Subsequently ~100 animals from each sex, split approximately evenly into 6, 12, and 18 month-aged groups, were randomly selected for total heart collection, which were then flash-frozen. Frozen heart samples were pulverized and aliquoted for RNA-seq and shotgun mass spectrometry for 192 of the samples with approximately equal representation of both sexes and age groups. The Jackson laboratory's Institutional Animal Care and Use Committee approved all the experiments used in this study.

Bulk RNA extraction

The total heart samples were lysed in Ambion TRIzol reagent (Thermo Fisher Scientific #15596026, Waltham, Massachusetts). Bulk RNA was isolated using the miRNeasy Mini kit (Qiagen Inc. #217004, Germantown, MD), according to the manufacture's protocols with the DNase digest step. RNA concentration and quality ratios were assessed using the Nanodrop 2000 spectrophotometer (Thermo Fisher Scientific) and RNA 600 Nano LabChip assay (Aligent Technologies, Santa Clara, CA).

RNA sequencing and quantification

Poly(A) RNA-seq libraries were generated using the TruSeq Stranded mRNA Library Prep Kit (Illumina, San Diego, CA). Libraries were pooled and sequenced 100 bp single-end on the HiSeq 2500 (Illumina) using TruSeq SBS Kit v4 reagents (Illumina).

Expectation-Maximization algorithm for Allele Specific Expression (EMASE) was used to quantify multi-parent allele-specific and total expression from RNA-seq data (120) using the Genotype by RNA-seq (GBRS) software package (https://gbrs.readthedocs.io/en/latest/).

Transcripts were removed if they did not have at least one read in at least half of the samples, resulting in a total of 20,932 transcripts for further analysis.

Protein quantification

Tissue from the total heart samples were homogenized in 1 ml lysis buffer, which consisted of 1% SDS, 50 mM Tris, pH 8.8 and Roche complete protease inhibitor cocktail (Roche # 11697498001, Clifton, NJ), and analyzed as previously described (74). Protein abundances were estimated from their component peptides identified through mass-spectrometry (MS) followed by a database search of MS spectra. Prior to protein abundance estimation, we filtered out peptides that contained polymorphisms relative to the mouse reference genome in order to minimize false pQTL signals that can occur due to failure to detect polymorphic peptides.

To estimate and normalize protein abundance from component peptides, we followed Huttlin et al. (2010) (121) and calculated:

Equation 1

$$\text{Protein}_{ij} = \log_2\left(\frac{\sum_K \text{Peptide}_{ik}}{s_i} + 1\right)$$

where K represents the set of observed peptides that map to protein j for mouse i and s_i is a scaling factor for standardizing samples within a batch. $s_i = \frac{\sum_L \text{Peptide}_{il}}{\max(\sum_L \text{Peptide}_{ql} \,|_{q \in b[i]})}$, where L is the set of all peptides observed for a sample, $b[i]$ denotes the batch of sample i, and $\max(\sum_L \text{Peptide}_{ql} : Q \in b[i])$ is the maximum sum of peptides for all the samples in batch $b[i]$. Protein abundance levels that were missing (NA) were imputed to be zero. Proteins with zeros for more than half the samples, resulting in a total of 4,062 proteins for further analysis.

The MS experiment was performed in batches of 10 samples processed and quantified simultaneously. Batch effects were removed using a linear mixed effect model (LMM) fit with the lme4 package (122). The batch effect, estimated as a best linear unbiased predictor (BLUP), was subtracted from each protein abundance, while age (as a categorical variable with three levels) and sex were included as fixed effect covariates in the model.

Differential transcript expression analysis by age

We used the DESeq2 package (123) to test for transcripts whose expression changed with age. Briefly, we fit the following generalized linear model (GLM) using the negative binomial distribution in DESeq2:

Equation 2

$$\mathrm{Transcript}_i = \mathrm{Sex}[i] + \mathrm{Gen}[i] + \mathrm{Age}[i]$$

where $\mathrm{Transcript}_i$ is the total count for each transcript from mouse i, $\mathrm{Sex}[i]$ is the effect corresponding to the sex of mouse i, $\mathrm{Gen}[i]$ is the effect corresponding to the generation of mouse i, and $\mathrm{Age}[i]$ is the effect corresponding to the age of mouse i, fit as a continuous variable at the month scale (6, 12, 18). The effect of age was tested using its Wald statistic. Transcripts with a significant age effect on expression were determined after FDR adjustment to account for multiple testing (FDR < 0.1).

Differential protein abundance analysis by age

To detect proteins with age effects, we fit a log-normal linear model with predictors similar to Equation 2:

Equation 3

$$\mathrm{Protein}_i = \mathrm{Sex}[i] + \mathrm{Gen}[i] + \mathrm{Age}[i] + \varepsilon_i$$

where $\mathrm{Protein}_i$ is the log-scale abundance of each protein from mouse i, as defined in Equation 1, ε_i is the residual, and all other terms as previously defined. Proteins with significant age effects were identified after FDR adjustment (FDR < 0.05).

Age trends in the correlation of genes coding for protein-complexes

To investigate the stoichiometry of known protein complexes (71) (CORUM database) we adapted a method described in McKenzie et al (2016) (17). We computed the Pearson correlation between the expression of each gene-pairs members of the protein complexes for both transcript and protein, at each age group. Then for each protein complex and data type (transcript and protein), we regressed the correlation coefficients of each gene-pair on age and recorded the slope, as exemplified in Equation 4:

Equation 4

$$\text{Correlation}_k^{i,j} = intercept + Age[k] + \varepsilon_k$$

Where $\text{Correlation}_k^{i,j}$ is the correlation between proteins i and j at age k, $intercept$ is the overall intercept, Age is the age effect, fit from a continuous encoding of age, $Age[k] = \beta_{Age} * k$, and ε_k is the residual at age k. In order to determine significance, we shuffled the mouse IDs and repeated the slope estimation 1,000 times to obtain FDR estimates using the DGCA package (17). Significant age-trends were declared at FDR < 0.1.

We also fit a model to compute the overall age trend for each protein complex, without fitting separate models per gene-pair. We fit a linear mixed model using the R/lme4 package to jointly model gene-pairs with a random effect, allowing the intercept and age slope for each gene-pair:

Equation 5

$$\text{Correlation}_{ijk} = \mu + u[ij] + (\beta_{\text{Age}} + v_{\text{Age}}[ij])x_k + \varepsilon_{ijk}$$

where Correlation_{ijk} is the correlation between proteins i and j at age k, μ is the overall intercept, $u[ij]$ is the random deviation on the intercept specific to the pairing of proteins i and j, β_{Age} is the overall age effect, $v_{\text{Age}}[ij]$ is the random deviation on the age effect specific to the paring of proteins i and j, x_k is the age (6, 12, or 18 months), and ε_{ijk} is random noise on the correlation for proteins i and j at age x_k. The protein pair-specific random terms are modeled as $\mathbf{u} \sim \text{N}(\mathbf{0}, \mathbf{I}\tau^2)$ and $\mathbf{v}_{\text{Age}} \sim \text{N}(\mathbf{0}, \mathbf{I}\tau^2_{\text{Age}})$, and the error as $\varepsilon_{ijk} \sim \text{N}(\mathbf{0}, \mathbf{I}\sigma^2)$. We also used the permutations procedure from McKenzie et al (2016) to determine significance, using a *p*-value cut-off of 0.05.

Additive QTL mapping

Although the results of additive QTL mapping are not reported here, it is useful to describe the methods used as a prelude to the description of age-interactive QTL mapping analysis. For each transcript or protein, we transformed the data to rank-normal scores and fit the following model at ~64,000 equally spaced loci across the genome:

Equation 6

$$\text{y}_{ij} = \text{QTL}_m[\text{i}] + \text{Sex}[i] + \text{Age}[i] + u_{mij} + \varepsilon_{ij}$$

where y_{ij} is the transcript or protein j expression/abundance for mouse i, $\mathrm{QTL}_m[\mathrm{i}]$ is the expected dosage of founder haplotype alleles for mouse i at locus m, u_{mij} is a random kinship effect that accounts for the correlation between individual DO mice due to shared genetic effects excluding the chromosome of locus m. The kinship effect is modeled as $\mathbf{u} \sim \mathrm{N}(\mathbf{0}, \mathbf{K}\tau_{\mathrm{K}}^2)$, where $\mathbf{K}$ is a realized genomic relationship matrix and τ_{K}^2 is the variance component underlying the kinship effect (124). The $\log_{10}$ likelihood ratio (LOD score) was determined by comparing the QTL model (Equation 4) to the null model without the QTL term.

Age-interactive QTL mapping

We performed a second set of genome scans to identify age-interactive QTL loci where the rate or direction of change of a transcript or protein is dependent on genotype. Genome scans for age-QTL are based on the following model:

Equation 7

$$y_{ij} = \mathrm{QTL}_{m[\mathrm{i}]} \times \mathrm{Age}[\mathrm{i}] + \mathrm{QTL}_m[\mathrm{i}] + \mathrm{Sex}[i] + \mathrm{Age}[i] + u_{mij} + \varepsilon_{ij}$$

where $\mathrm{QTL}_m \times \mathrm{Age}[\mathrm{i}]$ is the interaction effect between the QTL genotype and age of mouse i. All other terms are as previously defined. The null model for the age-interactive genome scans is the model from Equation 4, thus only the interaction term is being tested. To determine significance thresholds for age-QTL we required a more elaborate permutation procedure than the standard used for additive QTL (125). For each transcript or protein, we fit the following model:

Equation 8

$$y_{ij} = \mathrm{Sex}[i] + \mathrm{Age}[i] + u_{ij} + \varepsilon_{ij}$$

Where the kinship term u_{ij} includes effects of all loci, including the additive effect of the locus under evaluation. We then computed the residuals by subtracting the fitted values of model predictors:

Equation 7

$$e_{ij} = y_{ij} - \widehat{\mathrm{Sex}[\mathrm{i}]} + \widehat{\mathrm{Age}[\mathrm{i}]} + \widehat{u_{ij}}$$

To construct a permutation test, we generate null data by summing the fitted effect values with a randomly permutated of the residuals from Equation 7. We repeated the age-interactive scans on the residual-permuted phenotypes 1000 times to obtain a null distribution sample of the $\mathrm{LOD}_{\mathrm{int}}$ statistic. Signficance thresholds for the maximum $\mathrm{LOD}_{\mathrm{int}}$ scores were based on the 95th percentile of this

distribution and a suggestive threshold was determined using the 37th percentile. Transcript and protein age-QTLs were considered significant when LOD_{int} > 7.75 and suggestive when LOD_{int} > 6.0. All QTL analyses were performed with the R/qtl2 package (126).

Distal QTL hotspot analysis

Using a sliding window of 4 Mb, we counted the density of suggestive age-QTL (LOD_{int} > 6) for transcripts and proteins (Figure 4). We defined a genomic region as a hotspot based on having more than 40 age-QTLs. We used the hotspots to defines sets of transcripts and proteins that mapped to these regions. We further refined the hotspot sets by filtering out transcripts or proteins with a mean Pearson correlation coefficient < 0.3 with the other hotspot members, removing genes that were inconsistent with other members of the hotspot.

Age-specific allele effects

Transcripts or proteins with shared genetic drivers, which could cause distal age-QTL hotspots, should have similar genetic effects. To investigate this, we computed the principal components (PC) from the refined hotspot transcripts/proteins. We then estimated age-specific allele effects for the PC1, and also for the specific transcripts and proteins at the hotspot position. We included age and sex as additive covariates, and categorical age as the interactive term in the model. Using this model, we estimated allele effects at the age-QTL specific to the three age groups.

Functional enrichment analysis

We performed functional enrichment analysis for transcript/protein sets defined by having significant age effects and the members of the refined distal age-QTL hotspots. We used the ClusterProfiler package (127) to identify enriched gene ontology terms (biological processes, cellular compartments and molecular functions) for each set. We used stringent (FDR < 0.05) and lenient (FDR < 0.1) cut-offs to defined enriched categories for reporting.

Software

All data analysis and figures were generated using R v3.6.0 with the following packages: tidyverse v1.3.0, dplyr v0.8.5, tibble v2.1.3, ggplot2 v3.3.0 and gridExtra v2.3. The R Scripts used for all the analysis performed on this work can be found on Github (https://github.com/isabelagyuricza/Aging_Heart_DO_analysis) and on Figshare (DOI: 10.6084/m9.figshare.12430094.v1).

Data access

The RNA fastq files can be found on on NCBI SRA repository under bioproject PRJNA510989. The mass spectrometry proteomics data have been deposited to the ProteomeXchange Consortium via the PRIDE partner repository (http://www.proteomexchange.org/ - accession number pending). Both raw and normalized transcript expression matrices, as well as the protein abundance data have been deposited to Figshare (10.6084/m9.figshare.12378077). Genotype data is deposited the DODb database (https://dodb.jax.org/). All data and QTL results are available for download and interactive analysis using the QTLViewer for user driven queries (https://churchilllab.jax.org/qtlviewer/JAC/DOHeart). Raw and normalized quantification of transcripts and proteins and the genotype data are included in the download in a Rdata format suitable for further analysis.

Acknowledgements

The authors gratefully acknowledge the contribution of Matthew Vincent in generating mapping data through the QTL Viewer web tool. We also thank Heidi Munger and all the staff from the Genome Technology Service at The Jackson Laboratory for expert assistance with the RNA-seq experiments described in this publication. This work was supported by the National Institutes of Health and The Jackson Laboratory Nathan Shock Center of Excellence in the Basic Biology of Aging (AG038070).

Author contributions

IGG and GAC wrote the manuscript. GAC and RK conceived, designed and supervised the mouse aging experiment and tissue collection. SCM carried out the transcriptomics analysis. JMC and SPG carried

out the mass-spectrometry analysis. IGG analyzed the data and created figures with contributions from GAC, GRK and AGD.

Supplemental material legends

Supplemental Figure 1. Heatmaps for the Pearson correlation coefficients between transcripts or proteins that mapped to the age-QTL hotspots. A) Correlations between transcripts that mapped to the chromosome 4 age-eQTL hotspot show that there is no evidence for correlation in this group of transcripts. B) Correlations between proteins that mapped to the chromosomes 3 (B1), 5 (B2) and 12 (B3) age-pQTLs hotspots identify tightly correlated groups of proteins (positive or negative) that are potentially regulated by shared genetic variation.

Supplemental Table 1. List of transcripts that significantly change with age.

Supplemental Table 2. List of proteins that significantly change with age.

Supplemental Table 3. List of gene-pairs members of age-related protein-complexes that have a significant (FDR < 0.1) change in their pairwise correlations with age at the transcript or at the protein level.

Supplemental Table 4. List of age-pQTLs and age-eQTLs that mapped at the identified hotspots and their overall mean expression/abundance correlation with the other transcripts/proteins on the hotspot.

REFERENCES

1. Chiao YA, Rabinovitch PS. The aging heart. Cold Spring Harb Perspect Med. 2015 Sep 1;5(9).

2. North BJ, Sinclair DA. The intersection between aging and cardiovascular disease. Vol. 110, Circulation Research. Circ Res; 2012. p. 1097–108.

3. Quarles EK, Dai DF, Tocchi A, Basisty N, Gitari L, Rabinovitch PS. Quality control systems in cardiac aging. Ageing Res Rev [Internet]. 2015;23(PA):101–15. Available from: http://dx.doi.org/10.1016/j.arr.2015.02.003

4. Stanley WC, Recchia FA, Lopaschuk GD. Myocardial substrate metabolism in the normal and failing heart. Vol. 85, Physiological Reviews. 2005. p. 1093–129.

5. Dai DF, Chen T, Johnson SC, Szeto H, Rabinovitch PS. Cardiac aging: From molecular mechanisms to significance in human health and disease [Internet]. Vol. 16, Antioxidants and Redox Signaling. Mary Ann Liebert, Inc.; 2012 [cited 2020 Aug 26]. p. 1492–536. Available from: /pmc/articles/PMC3329953/?report=abstract

6. Melzer D, Hurst AJ, Frayling T. Genetic Variation and Human Aging: Progress and Prospects. Journals Gerontol Ser A Biol Sci Med Sci [Internet]. 2007 Mar 1 [cited 2019 Mar 22];62(3):301–7. Available from: https://academic.oup.com/biomedgerontology/article-lookup/doi/10.1093/gerona/62.3.301

7. Lakatta EG, Levy D. Arterial and Cardiac Aging: Major Shareholders in Cardiovascular Disease Enterprises. Circulation [Internet]. 2003 Jan 7 [cited 2019 Jun 7];107(1):139–46. Available from: https://www.ahajournals.org/doi/10.1161/01.CIR.0000048892.83521.58

8. Singh PP, Demmitt BA, Nath RD, Brunet A. The Genetics of Aging: A Vertebrate Perspective [Internet]. Vol. 177, Cell. Cell Press; 2019 [cited 2020 Mar 17]. p. 200–20. Available from: https://linkinghub.elsevier.com/retrieve/pii/S0092867419302211

9. Svenson KL, Gatti DM, Valdar W, Welsh CE, Cheng R, Chesler EJ, et al. High-resolution genetic mapping using the mouse Diversity Outbred population. Genetics [Internet]. 2012 [cited 2020 Aug 26];190(2):437–47. Available from: /pmc/articles/PMC3276626/?report=abstract

10. López-Otín C, Blasco MA, Partridge L, Serrano M, Kroemer G. The hallmarks of aging. Vol. 153, Cell. Cell Press; 2013. p. 1194.

11. Waldera-Lupa DM, Kalfalah F, Florea AM, Sass S, Kruse F, Rieder V, et al. Proteome-wide analysis reveals an age-associated cellular phenotype of in situ aged human fibroblasts. Aging (Albany NY) [Internet]. 2014 [cited 2020 Aug 7];6(10):856–78. Available from: /pmc/articles/PMC4247387/?report=abstract

12. Bahar R, Hartmann CH, Rodriguez KA, Denny AD, Busuttil RA, Dollé MET, et al. Increased cell-to-cell variation in gene expression in ageing mouse heart. Nature [Internet]. 2006 Jun 22 [cited 2020 Aug 7];441(7096):1011–4. Available from: https://www.nature.com/articles/nature04844

13. Işıldak U, Somel M, Thornton JM, Dönertaş HM. Temporal changes in the gene expression heterogeneity during brain development and aging. Sci Rep [Internet]. 2020 Dec 1 [cited 2020 Aug 7];10(1):1–15. Available from: https://www.nature.com/articles/s41598-020-60998-0

14. Gonskikh Y, Polacek N. Alterations of the translation apparatus during aging and stress response. Mech Ageing Dev [Internet]. 2017 [cited 2020 Aug 7];1–0. Available from: www.elsevier.com/locate/mechagedev

15. Cellerino A, Ori A. What have we learned on aging from omics studies? [Internet]. Vol. 70, Seminars in Cell and Developmental Biology. Elsevier Ltd; 2017 [cited 2020 Aug 23]. p. 177–89. Available from: https://pubmed.ncbi.nlm.nih.gov/28630026/

16. Subramanian A, Tamayo P, Mootha VK, Mukherjee S, Ebert BL, Gillette MA, et al. Gene set enrichment analysis: A knowledge-based approach for interpreting genome-wide expression profiles. Proc Natl Acad Sci U S A [Internet]. 2005 Oct 25 [cited 2020 Aug 23];102(43):15545–50. Available from: www.pnas.orgcgidoi10.1073pnas.0506580102

17. McKenzie AT, Katsyv I, Song WM, Wang M, Zhang B. DGCA: A comprehensive R package for Differential Gene Correlation Analysis. BMC Syst Biol. 2016 Nov 15;10(1):1–25.

18. Gordon JW. Regulation of cardiac myocyte cell death and differentiation by myocardin. Mol Cell Biochem [Internet]. 2018 Jan 19 [cited 2019 Mar 29];437(1–2):119–31. Available from: http://www.ncbi.nlm.nih.gov/pubmed/28631251

19. Barger PM, Kelly DP. PPAR signaling in the control of cardiac energy metabolism. Vol. 10, Trends in Cardiovascular Medicine. 2000. p. 238–45.

20. Erol A. The functions of PPARs in aging and longevity [Internet]. Vol. 2007, PPAR Research.

Hindawi Limited; 2007 [cited 2020 Aug 12]. Available from: /pmc/articles/PMC2254525/?report=abstract

21. Toba H, de Castro Brás LE, Baicu CF, Zile MR, Lindsey ML, Bradshaw AD. Increased ADAMTS1 mediates SPARC-dependent collagen deposition in the aging myocardium. Am J Physiol Endocrinol Metab [Internet]. 2016 [cited 2019 Mar 29];310(11):E1027-35. Available from: http://www.ncbi.nlm.nih.gov/pubmed/27143554

22. Khan SS, Shah SJ, Strande JL, Baldridge AS, Klyachko E, Flevaris P, et al. Identification of a Novel Familial Fibrotic Cardiomyopathy with a Loss-of-Function Mutation in SERPINE1. J Card Fail [Internet]. 2017 Aug 1 [cited 2019 Mar 29];23(8):S3. Available from: https://linkinghub.elsevier.com/retrieve/pii/S1071916417302233

23. Münch J, Grivas D, González-Rajal Á, Torregrosa-Carrión R, de la Pompa JL. Notch signalling restricts inflammation and serpine1 expression in the dynamic endocardium of the regenerating zebrafish heart. Development [Internet]. 2017 Apr 15 [cited 2019 Mar 29];144(8):1425–40. Available from: http://www.ncbi.nlm.nih.gov/pubmed/28242613

24. Heath E, Tahri D, Andermarcher E, Schofield P, Fleming S, Boulter CA. Abnormal skeletal and cardiac development, cardiomyopathy, muscle atrophy and cataracts in mice with a targeted disruption of the Nov (Ccn3) gene. BMC Dev Biol [Internet]. 2008 Feb 20 [cited 2019 Mar 29];8(1):18. Available from: http://www.ncbi.nlm.nih.gov/pubmed/18289368

25. Li CL, Martinez V, He B, Lombet A, Perbal B. A role for CCN3 (NOV) in calcium signalling. Mol Pathol [Internet]. 2002 Aug [cited 2019 Mar 29];55(4):250–61. Available from: http://www.ncbi.nlm.nih.gov/pubmed/12147716

26. Chu G, Kranias EG. Phospholamban as a therapeutic modality in heart failure. Novartis Found Symp [Internet]. 2006 [cited 2019 Mar 29];274:156–71; discussion 172-5, 272–6. Available from: http://www.ncbi.nlm.nih.gov/pubmed/17019811

27. Hu Z, Liu F, Li M, He J, Huang J, Rao DC, et al. Associations of Variants in the CACNA1A and CACNA1C Genes With Longitudinal Blood Pressure Changes and Hypertension Incidence: The GenSalt Study. Am J Hypertens [Internet]. 2016 [cited 2019 Mar 29];29(11):1301–6. Available from: http://www.ncbi.nlm.nih.gov/pubmed/27418245

28. Lu B, Tigchelaar W, Ruifrok WPT, van Gilst WH, de Boer RA, Silljé HHW. DHRS7c , a novel

cardiomyocyte-expressed gene that is down-regulated by adrenergic stimulation and in heart failure. Eur J Heart Fail [Internet]. 2012 Jan 1 [cited 2019 Mar 29];14(1):5–13. Available from: http://doi.wiley.com/10.1093/eurjhf/hfr152

29. Chen J, Sadowski HB, Kohanski RA, Wang L-H. Stat5 is a physiological substrate of the insulin receptor. Proc Natl Acad Sci U S A [Internet]. 1997 [cited 2019 Mar 29];94(6):2295. Available from: https://www.ncbi.nlm.nih.gov/pmc/articles/PMC20081/

30. Storz P, Döppler H, Pfizenmaier K, Müller G. Insulin selectively activates STAT5b, but not STAT5a, via a JAK2-independent signalling pathway in Kym-1 rhabdomyosarcoma cells. FEBS Lett [Internet]. 1999 Dec 31 [cited 2019 Mar 29];464(3):159–63. Available from: https://www.sciencedirect.com/science/article/pii/S0014579399016890

31. Grigorov I, Lazić T, Cvetković I, Milosavljević T, Petrović M. Opposite nuclear level and binding activity of STAT5B and STAT3 proteins with rat haptoglobin gene under normal and turpentine induced acute phase conditions. Mol Biol Rep. 2001 Dec 1;28(4):217–22.

32. Kang MJ, Yang S, Baek JW, Shim YS, Oh YJ, Hwang IT. Fetuin-A as an Alternative Marker for Insulin Resistance and Cardiovascular Risk in Prepubertal Children. J Atheroscler Thromb. 2017;

33. Westenfeld R, Schäfer C, Krüger T, Haarmann C, Schurgers LJ, Reutelingsperger C, et al. Fetuin-A protects against atherosclerotic calcification in CKD. J Am Soc Nephrol [Internet]. 2009 Jun [cited 2020 Aug 12];20(6):1264–74. Available from: /pmc/articles/PMC2689898/?report=abstract

34. Lindman BR, Clavel M-A, Mathieu P, Iung B, Lancellotti P, Otto CM, et al. Calcific aortic stenosis. Nat Rev Dis Prim [Internet]. 2016 [cited 2019 Mar 29];2:16006. Available from: http://www.ncbi.nlm.nih.gov/pubmed/27188578

35. Berkholz J, Zakrzewicz A, Munz B. skNAC depletion stimulates myoblast migration and perturbs sarcomerogenesis by enhancing calpain 1 and 3 activity. Biochem J [Internet]. 2013 Jul 15 [cited 2019 Mar 29];453(2):303–10. Available from: http://www.ncbi.nlm.nih.gov/pubmed/23662692

36. Munz B, Wiedmann M, Lochmüller H, Werner S. Cloning of novel injury-regulated genes. Implications for an important role of the muscle-specific protein skNAC in muscle repair. J Biol Chem [Internet]. 1999 May 7 [cited 2019 Mar 29];274(19):13305–10. Available from: http://www.ncbi.nlm.nih.gov/pubmed/10224091

37. Yotov W V, St-Arnaud R. Differential splicing-in of a proline-rich exon converts alphaNAC into a muscle-specific transcription factor. Genes Dev [Internet]. 1996 Jul 15 [cited 2019 Mar 29];10(14):1763–72. Available from: http://www.ncbi.nlm.nih.gov/pubmed/8698236

38. Howroyd P, Swanson C, Dunn C, Cattley RC, Corton JC. Decreased Longevity and Enhancement of Age-Dependent Lesions in Mice Lacking the Nuclear Receptor Peroxisome Proliferator-Activated Receptor α (PPARα). Toxicol Pathol [Internet]. 2004 Aug 2 [cited 2019 Mar 29];32(5):591–9. Available from: http://www.ncbi.nlm.nih.gov/pubmed/15603543

39. Yuan J, Mo H, Luo J, Zhao S, Liang S, Jiang Y, et al. PPARα activation alleviates damage to the cytoskeleton during acute myocardial ischemia/reperfusion in rats. Mol Med Rep [Internet]. 2018 Mar 16 [cited 2019 Mar 29];17(5):7218–26. Available from: http://www.ncbi.nlm.nih.gov/pubmed/29568903

40. Zhang Y-F, Xu H-M, Yu F, Wang M, Li M-Y, Xu T, et al. Crosstalk between MicroRNAs and Peroxisome Proliferator-Activated Receptors and Their Emerging Regulatory Roles in Cardiovascular Pathophysiology. PPAR Res [Internet]. 2018 Dec 5 [cited 2019 Mar 29];2018:1–11. Available from: http://www.ncbi.nlm.nih.gov/pubmed/30622558

41. Shi N, Li C-X, Cui X-B, Tomarev SI, Chen S-Y. Olfactomedin 2 Regulates Smooth Muscle Phenotypic Modulation and Vascular Remodeling Through Mediating Runx2 Binding to SRF Correspondence to. Arter Thromb Vasc Biol [Internet]. 2017 [cited 2019 Mar 29];37(3):446–54. Available from: http://www.gtexportal.org/home/gene/

42. Vassort G, Talavera K, Alvarez JL. Role of T-type Ca2+ channels in the heart. Cell Calcium. 2006;40(2):205–20.

43. Ferron L, Capuano V, Ruchon Y, Deroubaix E, Coulombe A, Renaud J-F. Angiotensin II Signaling Pathways Mediate Expression of Cardiac T-Type Calcium Channels. 2003 [cited 2020 Jan 27]; Available from: http://www.circresaha.org

44. Xia P, Liu Y, Cheng Z. Signaling Pathways in Cardiac Myocyte Apoptosis. Biomed Res Int [Internet]. 2016 [cited 2019 Mar 29];2016:9583268. Available from: http://www.ncbi.nlm.nih.gov/pubmed/28101515

45. Vincent B, De Bock K, Ramaekers M, Van Den Eede E, Van Leemputte M, Hespel P, et al. ACTN3 (R577X) genotype is associated with fiber type distribution. Physiol Genomics. 2007 Dec

19;32(1):58–63.

46. MacArthur DG, Seto JT, Raftery JM, Quinlan KG, Huttley GA, Hook JW, et al. Loss of ACTN3 gene function alters mouse muscle metabolism and shows evidence of positive selection in humans. Nat Genet. 2007 Oct;39(10):1261–5.

47. Muslin AJ. Akt2: A critical regulator of cardiomyocyte survival and metabolism. In: Pediatric Cardiology. 2011. p. 317–22.

48. Pillai VB, Sundaresan NR, Gupta MP. Regulation of Akt signaling by sirtuins: its implication in cardiac hypertrophy and aging. Circ Res [Internet]. 2014 Jan 17 [cited 2020 Aug 12];114(2):368–78. Available from: http://www.ncbi.nlm.nih.gov/pubmed/24436432

49. DeBosch B, Treskov I, Lupu TS, Weinheimer C, Kovacs A, Courtois M, et al. Akt1 is required for physiological cardiac growth. Circulation. 2006 May;113(17):2097–104.

50. DeBosch B, Sambandam N, Weinheimer C, Courtois M, Muslin AJ. Akt2 regulates cardiac metabolism and cardiomyocyte survival. J Biol Chem. 2006 Oct 27;281(43):32841–51.

51. Essop MF, Camp HS, Cheol SC, Sharma S, Fryer RM, Reinhart GA, et al. Reduced heart size and increased myocardial fuel substrate oxidation in ACC2 mutant mice. Am J Physiol - Hear Circ Physiol. 2008 Jul;295(1).

52. Kaslow HR, Lesikar DD. Isozymes of glycogen synthase. FEBS Lett. 1984 Jul 9;172(2):294–8.

53. Wu G, Yussman MG, Barrett TJ, Hahn HS, Osinska H, Hilliard GM, et al. Increased Myocardial Rab GTPase Expression A Consequence and Cause of Cardiomyopathy. 2001 [cited 2020 Jan 30]; Available from: http://www.circresaha.org

54. Martinez O, Goud B. Rab proteins. Biochim Biophys Acta - Mol Cell Res. 1998 Aug 14;1404(1–2):101–12.

55. Yamano K, Wang C, Sarraf SA, Münch C, Kikuchi R, Noda NN, et al. Endosomal rab cycles regulate parkin-mediated mitophagy. Elife. 2018 Jan 23;7.

56. Touchot N, Zahraoui A, Vielh E, Tavitian A. Biochemical properties of the YPT-related rab1B protein. Comparison with rab1A. FEBS Lett. 1989 Oct 9;256(1–2):79–84.

57. Wei TC, Lin HY, Lu CC, Chen CM, You LR. Expression of Crip2, a LIM-domain-only protein, in the

mouse cardiovascular system under physiological and pathological conditions. Gene Expr Patterns. 2011 Oct;11(7):384–94.

58. Sun X, Zhang R, Lin X, Xu X. Wnt3a regulates the development of cardiac neural crest cells by modulating expression of cysteine-rich intestinal protein 2 in rhombomere 6. Circ Res [Internet]. 2008 Apr 11 [cited 2020 Jan 28];102(7):831–9. Available from: http://www.ncbi.nlm.nih.gov/pubmed/18292601

59. Trembinski DJ, Bink DI, Theodorou K, Sommer J, Fischer A, van Bergen A, et al. Aging-regulated anti-apoptotic long non-coding RNA Sarrah augments recovery from acute myocardial infarction. Nat Commun [Internet]. 2020 Dec 1 [cited 2020 Aug 12];11(1):1–14. Available from: https://doi.org/10.1038/s41467-020-15995-2

60. Chen WW, Birsoy K, Mihaylova MM, Snitkin H, Stasinski I, Yucel B, et al. Inhibition of ATPIF1 ameliorates severe mitochondrial respiratory chain dysfunction in mammalian cells. Cell Rep. 2014 Oct 4;7(1):27–34.

61. Lefebvre V, Du Q, Baird S, Ng ACH, Nascimento M, Campanella M, et al. Genome-wide RNAi screen identifies ATPase inhibitory factor 1 (ATPIF1) as essential for PARK2 recruitment and mitophagy. Autophagy. 2013;9(11):1770–9.

62. Callegari S, Richter F, Chojnacka K, Jans DC, Lorenzi I, Pacheu-Grau D, et al. TIM29 is a subunit of the human carrier translocase required for protein transport. Vol. 590, FEBS Letters. Wiley Blackwell; 2016. p. 4147–58.

63. Ohta S, Goto K, Arai H, Kagawa Y. An extremely acidic amino-terminal presequence of the precursor for the human mitochondrial hinge protein. FEBS Lett. 1987 Dec 21;226(1):171–5.

64. Hirawake H, Taniwaki M, Tamura A, Kojima S, Kita K. Cytochrome win human complex II (succinate-ubiquinoneoxidoreductase): cDNA cloning of the components in liver mitochondria and chromosome assignment of the genes for the large (SDHC) and small (SDHD) subunitsto 1q21 and 11q23. Cytogenet Genome Res [Internet]. 1997 Jan 1 [cited 2020 Mar 26];79(1–2):132–8. Available from: https://www.karger.com/Article/FullText/134700

65. Zeviani M, Masanori N, Herbert J, Lomax MI, Grossman LI, Sherbany AA, et al. Isolation of a cDNA clone encoding subunit IV of human cytochrome c oxidase. Gene. 1987 Jan 1;55(2–3):205–17.

66. Loeffen JLCM, Triepels RH, Van Den Heuvel LP, Schuelke M, Buskens CAF, Smeets RJP, et al. cDNA of eight nuclear encoded subunits of NADH:ubiquinone oxidoreductase: Human complex I cDNA characterization completed. Biochem Biophys Res Commun [Internet]. 1998 Dec 18 [cited 2020 Mar 26];253(2):415–22. Available from: https://linkinghub.elsevier.com/retrieve/pii/S0006291X98997868

67. Loublier S, Bayot A, Rak M, El-Khoury R, Bénit P, Rustin P. The NDUFB6 subunit of the mitochondrial respiratory chain complex I is required for electron transfer activity: A proof of principle study on stable and controlled RNA interference in human cell lines. Biochem Biophys Res Commun. 2011 Oct 22;414(2):367–72.

68. Zhuchenko O, Wehnert M, Bailey J, Zhong SS, Cheng CL. Isolation, mapping, and genomic structure of an X-linked gene for a subunit of human mitochondrial complex I. Genomics. 1996 Nov 1;37(3):281–8.

69. Anisimova AS, Alexandrov AI, Makarova NE, Gladyshev VN, Dmitriev SE. Protein synthesis and quality control in aging. Vol. 10, Aging. Impact Journals LLC; 2018. p. 4269–88.

70. Taggart JC, Zauber H, Selbach M, Li GW, McShane E. Keeping the Proportions of Protein Complex Components in Check. Vol. 10, Cell Systems. Cell Press; 2020. p. 125–32.

71. Giurgiu M, Reinhard J, Brauner B, Dunger-Kaltenbach I, Fobo G, Frishman G, et al. CORUM: the comprehensive resource of mammalian protein complexes-2019. Nucleic Acids Res [Internet]. 2019 [cited 2020 Apr 28];47:559–63. Available from: http://mips.helmholtz-muenchen.de/corum/.

72. Yao C, Chen G, Song C, Keefe J, Mendelson M, Huan T, et al. Genome-wide mapping of plasma protein QTLs identifies putatively causal genes and pathways for cardiovascular disease. Nat Commun [Internet]. 2018 Dec 1 [cited 2020 Aug 23];9(1):1–11. Available from: www.nature.com/naturecommunications

73. Hause RJ, Stark AL, Antao NN, Gorsic LK, Chung SH, Brown CD, et al. Identification and validation of genetic variants that influence transcription factor and cell signaling protein levels. Am J Hum Genet [Internet]. 2014 Aug 7 [cited 2020 Aug 23];95(2):194–208. Available from: http://dx.doi.org/10.1016/j.ajhg.2014.07.005.

74. Chick JM, Munger SC, Simecek P, Huttlin EL, Choi K, Daniel M. Defining the consequences of

genetic variation on a proteome-wide scale. Nature [Internet]. 2016;002801:1–39. Available from: http://dx.doi.org/10.1038/nature18270

75. Albert FW, Bloom JS, Siegel J, Day L, Kruglyak L. Genetics of trans-regulatory variation in gene expression. Elife [Internet]. 2018 Jul 17 [cited 2020 Jul 17];7. Available from: /pmc/articles/PMC6072440/?report=abstract

76. Battle A, Khan Z, Wang SH, Mitrano A, Ford MJ, Pritchard JK, et al. Impact of regulatory variation from RNA to protein. Science (80-) [Internet]. 2015 Feb 6 [cited 2020 Aug 23];347(6222):664–7. Available from: https://pubmed.ncbi.nlm.nih.gov/25657249/

77. Gao J, Schatton D, Martinelli P, Hansen H, Pla-Martin D, Barth E, et al. CLUH regulates mitochondrial biogenesis by binding mRNAs of nuclear-encoded mitochondrial proteins. J Cell Biol. 2014;207(2):213–23.

78. Schatton D, Pla-Martin D, Marx MC, Hansen H, Mourier A, Nemazanyy I, et al. CLUH regulates mitochondrial metabolism by controlling translation and decay of target mRNAs. J Cell Biol. 2017 Mar 6;216(3):675–93.

79. Billia F, Hauck L, Grothe D, Konecny F, Rao V, Kim RH, et al. Parkinson-susceptibility gene DJ-1/PARK7 protects the murine heart from oxidative damage in vivo. Proc Natl Acad Sci U S A [Internet]. 2013 Apr 9 [cited 2020 Jun 30];110(15):6085–90. Available from: https://pubmed.ncbi.nlm.nih.gov/23530187/

80. Sarikhani M, Maity S, Mishra S, Jain A, Tamta AK, Ravi V, et al. SIRT2 deacetylase represses NFAT transcription factor to maintain cardiac homeostasis. J Biol Chem. 2018 Apr 6;293(14):5281–94.

81. Tang X, Chen XF, Wang NY, Wang XM, Liang ST, Zheng W, et al. SIRT2 acts as a cardioprotective deacetylase in pathological cardiac hypertrophy. Circulation [Internet]. 2017 Nov 1 [cited 2020 Jun 30];136(21):2051–67. Available from: /pmc/articles/PMC5698109/?report=abstract

82. Takahashi Y, Coppola D, Matsushita N, Cualing HD, Sun M, Sato Y, et al. Bif-1 interacts with Beclin 1 through UVRAG and regulates autophagy and tumorigenesis. Nat Cell Biol [Internet]. 2007 Oct [cited 2020 Jun 29];9(10):1142–51. Available from: https://pubmed.ncbi.nlm.nih.gov/17891140/

83. Takahashi Y, Meyerkord CL, Wang HG. Bif-1/Endophilin B1: A candidate for crescent driving force in autophagy [Internet]. Vol. 16, Cell Death and Differentiation. NIH Public Access; 2009 [cited

2020 Jun 29]. p. 947–55. Available from: /pmc/articles/PMC2697278/?report=abstract

84. Escobar KA, Cole NH, Mermier CM, VanDusseldorp TA. Autophagy and aging: Maintaining the proteome through exercise and caloric restriction [Internet]. Vol. 18, Aging Cell. Blackwell Publishing Ltd; 2019 [cited 2020 Jun 29]. Available from: https://onlinelibrary.wiley.com/doi/full/10.1111/acel.12876

85. Strait JB, Lakatta EG. Aging-Associated Cardiovascular Changes and Their Relationship to Heart Failure. Vol. 8, Heart Failure Clinics. NIH Public Access; 2012. p. 143–64.

86. Biernacka A, Frangogiannis NG. Aging and Cardiac Fibrosis. Vol. 2, Aging and Disease •. 2011.

87. Horn MA, Graham HK, Richards MA, Clarke JD, Greensmith DJ, Briston SJ, et al. Age-related divergent remodeling of the cardiac extracellular matrix in heart failure: Collagen accumulation in the young and loss in the aged. J Mol Cell Cardiol. 2012 Jul;53(1):82–90.

88. Sessions AO, Engler AJ. Mechanical Regulation of Cardiac Aging in Model Systems. Vol. 118, Circulation Research. Lippincott Williams and Wilkins; 2016. p. 1553–62.

89. Nishtala K, Phong TQ, Steil L, Sauter M, Salazar MG, Kandolf R, et al. Proteomic analyses of age related changes in A.BY/SnJ mouse hearts. Proteome Sci. 2013;11(1).

90. Chakravarti B, Oseguera M, Dalal N, Fathy P, Mallik B, Raval A, et al. Proteomic profiling of aging in the mouse heart: Altered expression of mitochondrial proteins. Arch Biochem Biophys [Internet]. 2008 Jun 1 [cited 2020 Aug 12];474(1):22–31. Available from: https://linkinghub.elsevier.com/retrieve/pii/S0003986108000556

91. Mills MA, Yang N, Weinberger RP, Woude DL Vander, Beggs AH, Easteal S, et al. Differential expression of the actin-binding proteins, α-actinin-2 and-3, in different species: implications for the evolution of functional redundancy [Internet]. Vol. 10, Human Molecular Genetics. 2001 [cited 2020 Mar 5]. Available from: http://www.ncbi.nlm.nih.gov/

92. Arvanitis M, Tampakakis E, Zhang Y, Wang W, Auton A, Dutta D, et al. Genome-wide association and multi-omic analyses reveal ACTN2 as a gene linked to heart failure. Nat Commun [Internet]. 2020 Dec 28 [cited 2020 Mar 5];11(1):1122. Available from: http://www.nature.com/articles/s41467-020-14843-7

93. Rajabi M, Kassiotis C, Razeghi P, Taegtmeyer H. Return to the fetal gene program protects the

stressed heart: A strong hypothesis. Heart Fail Rev [Internet]. 2007 Dec 19 [cited 2020 Feb 28];12(3–4):331–43. Available from: http://link.springer.com/10.1007/s10741-007-9034-1

94. Taegtmeyer H, Sen S, Vela D. Return to the fetal gene program: A suggested metabolic link to gene expression in the heart. In: Annals of the New York Academy of Sciences [Internet]. Blackwell Publishing Inc.; 2010 [cited 2020 Jun 30]. p. 191–8. Available from: /pmc/articles/PMC3625436/?report=abstract

95. Korvald C, Elvenes OP, Myrmel T. Myocardial substrate metabolism influences left ventricular energetics in vivo. Am J Physiol - Hear Circ Physiol. 2000;278(4 47-4).

96. Yeo EJ. Hypoxia and aging. Vol. 51, Experimental and Molecular Medicine. Nature Publishing Group; 2019. p. 1–15.

97. Moreno Rosa C, Priscilla Xavier N, Henrique Campos D, Angélica Henrique Fernandes A, Diarcadia Mariano Cezar M, Felippe Martinez P, et al. Diabetes mellitus activates fetal gene program and intensifies cardiac remodeling and oxidative stress in aged spontaneously hypertensive rats [Internet]. Vol. 12, Cardiovascular Diabetology. 2013 [cited 2020 Feb 28]. Available from: http://www.cardiab.com/content/12/1/152

98. Connelly KA, Kelly DJ, Zhang Y, Prior DL, Advani A, Cox AJ, et al. Inhibition of protein kinase C-β by ruboxistaurin preserves cardiac function and reduces extracellular matrix production in diabetic cardiomyopathy. Circ Hear Fail [Internet]. 2009 Mar [cited 2020 Feb 28];2(2):129–37. Available from: http://www.ncbi.nlm.nih.gov/pubmed/19808328

99. Kelmer Sacramento E, Kirkpatrick JM, Mazzetto M, Di S, Caterino C, Sanguanini M, et al. Reduced proteasome activity in the aging brain results in ribosome stoichiometry loss and aggregation. BioRxiv [Internet]. 2019 [cited 2020 Apr 10];1–25. Available from: https://doi.org/10.1101/577478

100. Walther DM, Kasturi P, Zheng M, Pinkert S, Vecchi G, Ciryam P, et al. Widespread proteome remodeling and aggregation in aging C. elegans. Cell. 2015 May 7;161(4):919–32.

101. Janssens GE, Meinema AC, González J, Wolters JC, Schmidt A, Guryev V, et al. Protein biogenesis machinery is a driver of replicative aging in yeast. Elife. 2015 Dec 1;4(September 2015).

102. Harper JW, Bennett EJ. Proteome complexity and the forces that drive proteome imbalance. Vol.

537, Nature. Nature Publishing Group; 2016. p. 328–38.

103. Carrard G, Bulteau AL, Petropoulos I, Friguet B. Impairment of proteasome structure and function in aging. Vol. 34, International Journal of Biochemistry and Cell Biology. Pergamon; 2002. p. 1461–74.

104. Higuchi-Sanabria R, Frankino PA, Paul JW, Tronnes SU, Dillin A. A Futile Battle? Protein Quality Control and the Stress of Aging [Internet]. Vol. 44, Developmental Cell. Cell Press; 2018 [cited 2020 Jun 30]. p. 139–63. Available from: https://pubmed.ncbi.nlm.nih.gov/29401418/

105. Belmont PJ, Tadimalla A, Chen WJ, Martindale JJ, Thuerauf DJ, Marcinko M, et al. Coordination of Growth and Endoplasmic Reticulum Stress Signaling by Regulator of Calcineurin 1 (RCAN1), a Novel ATF6-inducible Gene * □ S. 2008 [cited 2019 Dec 19]; Available from: http://www.jbc.org

106. Szegezdi E, Logue SE, Gorman AM, Samali A. Mediators of endoplasmic reticulum stress-induced apoptosis. Vol. 7, EMBO Reports. European Molecular Biology Organization; 2006. p. 880–5.

107. Martindale JJ, Fernandez R, Thuerauf D, Whittaker R, Gude N, Sussman MA, et al. Endoplasmic reticulum stress gene induction and protection from ischemia/reperfusion injury in the hearts of transgenic mice with a tamoxifen-regulated form of ATF6. Circ Res. 2006 May;98(9):1186–93.

108. Toko H, Takahashi H, Kayama Y, Okada S, Minamino T, Terasaki F, et al. ATF6 is important under both pathological and physiological states in the heart. J Mol Cell Cardiol. 2010 Jul;49(1):113–20.

109. Ishimi Y, Kojima M, Takeuchi F, Miyamoto T, Yamada MA, Hanaoka F. Changes in chromatin structure during aging of human skin fibroblasts. Exp Cell Res. 1987;169(2):458–67.

110. Smeal T, Claus J, Kennedy B, Cole F, Guarente L. Loss of transcriptional silencing causes sterility in old mother cells of S. cerevisiae. Cell. 1996 Feb 23;84(4):633–42.

111. Enright HU, Miller WJ, Hebbel RP. Nucleosomal histone protein protects DNA from iron-mediated damage. Vol. 20, Nucleic Acids Research.

112. Ljungman M, Hanawalt PC. Efficient protection against oxidative DNA damage in chromatin. Mol Carcinog. 1992;5(4):264–9.

113. Cuddeback SM, Yamaguchi H, Komatsu K, Miyashita T, Yamada M, Wu C, et al. Molecular cloning and characterization of Bif-1. A novel Src homology 3 domain-containing protein that associates with Bax. J Biol Chem [Internet]. 2001 Jun 8 [cited 2020 Jun 29];276(23):20559–65. Available

from: https://pubmed.ncbi.nlm.nih.gov/11259440/

114. Karbowski M, Jeong SY, Youle RJ. Endophilin B1 is required for the maintenance of mitochondrial morphology. J Cell Biol. 2004 Sep 27;166(7):1027–39.

115. Komatsu M, Waguri S, Chiba T, Murata S, Iwata JI, Tanida I, et al. Loss of autophagy in the central nervous system causes neurodegeneration in mice. Nature. 2006 Jun 15;441(7095):880–4.

116. Nakai A, Yamaguchi O, Takeda T, Higuchi Y, Hikoso S, Taniike M, et al. The role of autophagy in cardiomyocytes in the basal state and in response to hemodynamic stress. Nat Med. 2007 May;13(5):619–24.

117. Mathew R, Kongara S, Beaudoin B, Karp CM, Bray K, Degenhardt K, et al. Autophagy suppresses tumor progression by limiting chromosomal instability. Genes Dev [Internet]. 2007 Jun 1 [cited 2020 Jun 29];21(11):1367–81. Available from: /pmc/articles/PMC1877749/?report=abstract

118. Takahashi Y, Hori T, Cooper TK, Liao J, Desai N, Serfass JM, et al. Bif-1 haploinsufficiency promotes chromosomal instability and accelerates Myc-driven lymphomagenesis via suppression of mitophagy. Blood [Internet]. 2013 Feb 28 [cited 2020 Jun 29];121(9):1622–32. Available from: /pmc/articles/PMC3587325/?report=abstract

119. Taneike M, Yamaguchi O, Nakai A, Hikoso S, Takeda T, Mizote I, et al. Inhibition of autophagy in the heart induces age-related cardiomyopathy. Autophagy [Internet]. 2010 [cited 2020 Jun 29];6(5):600–6. Available from: https://www.tandfonline.com/action/journalInformation?journalCode=kaup20

120. Raghupathy N, Choi K, Vincent MJ, Beane GL, Sheppard KS, Munger SC, et al. Hierarchical analysis of RNA-seq reads improves the accuracy of allele-specific expression. Valencia A, editor. Bioinformatics [Internet]. 2018 Jul 1 [cited 2019 Jul 29];34(13):2177–84. Available from: https://academic.oup.com/bioinformatics/article/34/13/2177/4850941

121. Huttlin EL, Jedrychowski MP, Elias JE, Goswami T, Rad R, Beausoleil SA, et al. A tissue-specific atlas of mouse protein phosphorylation and expression. Cell [Internet]. 2010 Dec 23 [cited 2020 Jul 10];143(7):1174–89. Available from: /pmc/articles/PMC3035969/?report=abstract

122. Bates D, Mächler M, Bolker B, Walker S. Fitting Linear Mixed-Effects Models Using lme4. J Stat Softw. 2015;67(1).

123. Love MI, Huber W, Anders S. Moderated estimation of fold change and dispersion for RNA-seq data with DESeq2. Genome Biol [Internet]. 2014;15(12):550. Available from: http://genomebiology.biomedcentral.com/articles/10.1186/s13059-014-0550-8

124. Yang J, Zaitlen NA, Goddard ME, Visscher PM, Price AL. Advantages and pitfalls in the application of mixed-model association methods [Internet]. Vol. 46, Nature Genetics. Nature Publishing Group; 2014 [cited 2020 Aug 23]. p. 100–6. Available from: https://pubmed.ncbi.nlm.nih.gov/24473328/

125. Churchill GA, Doerge RW. Empirical threshold values for quantitative trait mapping. Genetics. 1994;138(3):963–71.

126. Broman KW, Gatti DM, Simecek P, Furlotte NA, Prins P, Sen Ś, et al. R/qtl2: Software for Mapping Quantitative Trait Loci with High-Dimensional Data and Multiparent Populations. Genetics [Internet]. 2019 Feb 1 [cited 2019 Mar 29];211(2):495–502. Available from: http://www.ncbi.nlm.nih.gov/pubmed/30591514

127. Yu G, Wang L-G, Han Y, He Q-Y. clusterProfiler: an R package for comparing biological themes among gene clusters. OMICS [Internet]. 2012 May [cited 2019 Mar 29];16(5):284–7. Available from: http://www.ncbi.nlm.nih.gov/pubmed/22455463